VILNIUS TECH
Vilnius Gediminas Technical University

Journal of Civil Engineering and Management
ISSN 1392-3730 / eISSN 1822-3605
2021 Volume 27 Issue 2: 117–138
https://doi.org/10.3846/jcem.2021.14304

EMPIRICAL SHEAR BASED MODEL FOR PREDICTING PLATE END DEBONDING IN FRP STRENGTHENED RC BEAMS

Ahmed K. EL-SAYED[1], Mohammed A. AL-SAAWANI[1*], Abdulaziz I. AL-NEGHEIMISH[2]

[1]*Center of Excellence for Concrete Research and Testing, Civil Engineering Department, King Saud University, Riyadh, Saudi Arabia*
[2]*Civil Engineering Department, King Saud University, Riyadh, Saudi Arabia*

Received 18 June 2020; accepted 14 December 2020

Abstract. This paper presents the development of a simplified model for predicting plate end (PE) debonding capacity of reinforced concrete (RC) beams flexurally strengthened using fiber reinforced polymers (FRP). The proposed model is based on the concrete shear strength of the beams considering main parameters known to affect the opening of the shear cracks and consequently affect PE debonding. The model considers also the effect of the location of the cut-off point of FRP plate along the span of the beam. The proposed model was verified against experimental database of 128 FRP-strengthened beams collected from previous studies that failed in PE debonding. In addition, the predictions of the proposed model were also compared with those of the existing PE debonding models. The predictions of the model were found to be comparable to the best predictions provided by the existing models, yet the proposed model is simpler. Furthermore, the proposed model was combined with the ACI 440 IC debonding equation to provide a procedure for predicting the governing debonding failure mode in FRP strengthened RC beams. The procedure was validated against 238 beam tests available in the literature, and shown to be a reliable approach.

Keywords: beams, concrete, fiber-reinforced polymer, plate-end debonding, prediction model, strengthening.

Introduction

The use of fiber reinforced polymers (FRP) for strengthening reinforced concrete (RC) members has become popular in the engineering practice. This is attributed to the superior characteristics of FRP materials which make them more attractive to be used in repair and upgrade applications of existing concrete structures. FRP materials have a high strength to weight ratio as well as high immunity to corrosion according to ACI 440.2R (American Concrete Institute [ACI], 2017). Nevertheless, delamination of FRP reinforcement from the concrete surface represents one of the challenges that limits the full use of strain capacity of FRP materials in the design process. Reinforced concrete beams strengthened in flexure using FRP reinforcement generally fail either in intermediate-crack (IC) debonding or plate end (PE) debonding. The tensile strain developed in FRP reinforcement at the occurrence of any of such debonding failures represents a fraction of FRP ultimate tensile strain. Compared to beams failing in IC debonding, beams failing in PE debonding generally experience a lower FRP tensile strain at failure which makes PE debonding a more critical mode of failure (National Research Council, 2013; Al-Saawani et al., 2015).

PE debonding occurs in beams with relatively small shear span to depth ratio. Because in such beams, the bending moment is relatively small and the behavior is governed by shear not by flexure. This reduces the chance of the occurrence of IC debonding failure. PE debonding initiates at the FRP plate end propagating towards the midspan of the beam. It occurs as separation of the concrete cover at the level of main tensile steel or as interfacial debonding of the plate from the concrete of the beam soffit. The concrete cover separation (CCS) is more commonly to occur than the plate end interfacial debonding in FRP-strengthened RC beams. For beams with FRP terminated close to the support, CCS occurs after the formation of shear cracks at the plate end region (Oehlers, 1992; Smith & Teng, 2002a; Zhang & Teng, 2016; Achintha & Burgoyne, 2008, 2011). Shear cracks

*Corresponding author. E-mail: *malsaawani@ksu.edu.sa*

are inclined and associated with horizontal and vertical opening displacements between the two surfaces of the crack. Horizontal displacement induces interfacial shear stresses between FRP plate and the concrete surface. On the other hand, vertical displacement induces normal tensile stresses acting on the concrete cover between the FRP and the embedded tensile steel bars (International Federation for Structural Concrete [*fib*], 2001). Opening of the shear crack under loading will increase both horizontal and vertical displacements which in turn will increase both interfacial and normal stresses, respectively. In CCS failure, the normal tensile stresses are more critical than interfacial shear stresses. The increase of these stresses leads to the formation of horizontal splitting cracks at the level of the tensile reinforcing steel bars and separation of the concrete cover. The concrete cover with the bonded FRP plate separate as one unit as shown in Figure 1. For strengthened beams with FRP terminated away from the support, CCS occurs after the formation of inclined cracks that develop at the plate end and propagate in the beam towards the tension steel bars. Once the cracks reach the level of the steel bars, they propagate horizontally causing splitting of the concrete cover (Achintha & Burgoyne, 2008, 2011). Plate-end interfacial debonding occurs due to higher interfacial shear stresses near the FRP plate end, which are more critical than the normal stresses in this case. Debonding initiates at the end of the FRP plate when the interfacial stresses exceed the tensile strength of the concrete substrate. It propagates along the interface of concrete and FRP towards the middle of the beam without reaching the level of tension steel reinforcement, as shown in Figure 2. This debonding failure is most likely to occur when the FRP plate width is significantly narrower than the beam width (Zhang & Teng, 2016).

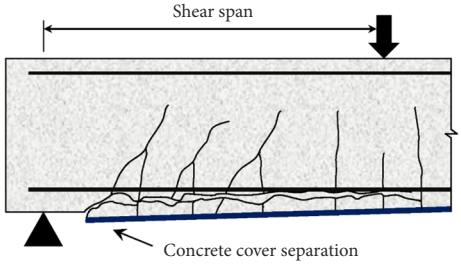

Figure 1. Concrete cover separation in FRP strengthened RC beams

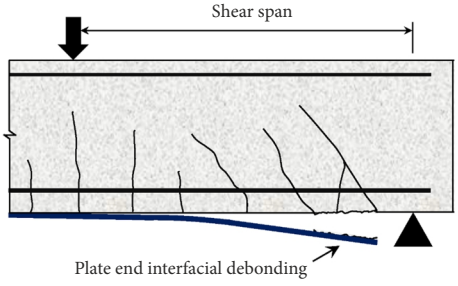

Figure 2. Plate end interfacial debonding in FRP strengthened RC beams

In addition to experimental studies, the topic of plate end debonding has attracted the researchers to conduct numerical investigations on FRP strengthened concrete beams using different finite element (FE) models. The studies suggested two-dimensional (2D) or three-dimensional (3D) models (e.g., Zhang & Teng, 2014; Kotynia et al., 2008; Sakr, 2018) to analyze plate-end interfacial debonding and concrete cover separation failures using different commercial FE packages.

The occurrence of PE debonding at lower FRP tensile strain diminishes the feasibility of using FRP external strengthening. To enhance the efficiency of FRP strengthening, end anchorage system should be provided to mitigate/prevent the premature PE debonding failure. To properly design such an end anchorage system, the PE debonding capacity of an FRP-strengthened beam should be reliably predicted first. The aim of this study is to develop a simplified model for predicting the plate end debonding in RC beams flexurally strengthened with FRP reinforcement. This paper presents the development of the model which is based on the concrete shear strength of RC beams. The beneficial effect of the shear reinforcement on restricting the widening of shear cracks and consequently increasing the PE debonding capacity is considered in the model. Also, the effect of the location of the termination point of FRP plate along the beam span is considered. The model is verified using experimental database collected from previous studies. In addition, the model is compared with the existing models in predicting the PE debonding capacity of FRP strengthened beams included in the database. The study is extended by combining the model with ACI 440.2R (ACI, 2017) IC debonding equation for predicting the governing debonding failure mode of FRP strengthened RC beams.

1. Overview of existing shear based models

There are several existing models for predicting PE debonding failure in FRP strengthened RC beams. Most of these models are based on shear strength of the beams or based on fracture mechanics. This section provides an overview of the shear based models as they represent the majority of the available models while other models based on fracture mechanics will be presented later in the paper in Section 6. A total of ten models proposed by researchers or recommended by relevant design codes and guidelines are presented. All the following equations are presented in SI unit format.

1.1. Oehlers' model

Earlier work was conducted by Oehlers (1992) and resulted in developing a strength model based on the shear force and bending moment acting at the plate end. Oehlers' work was carried out on RC beams strengthened with steel plates and yielded the following moment-shear interaction expression:

$$\frac{M_{db,end}}{M_{db,f}}+\frac{V_{db,end}}{V_{db,s}}\le 1.17 \text{ and}$$
$$M_{db,end}\le M_{db,f},\ V_{db,end}\le V_{db,s}, \quad (1)$$

where $M_{db,end}$ and $V_{db,end}$ are the bending moment and shear force applied at the plate end at failure, respectively. The term $M_{db,f}$ is the debonding moment at the end of a plate terminated in the constant moment region, whereas the term $V_{db,s}$ is the debonding shear force at the end of a plate terminated near the support.

Oehlers (1992) indicated that there are two extreme positions of soffit plate termination. For a plate terminated close to the supports in a simply supported beam, the applied moment $M_{db,end}$ at the plate end will be zero, and the PE debonding occurs when the applied shear force $V_{db,end}$ at the plate end reaches the concrete shear strength V_c of the beam. On the other hand, for a plate terminated in the constant moment region, the applied shear force $V_{db,end}$ at the plate end will be zero and the PE debonding occurs when the applied moment $M_{db,end}$ reaches $M_{db,f}$. The ultimate debonding moment $M_{db,f}$ is given by the following equation:

$$M_{db,f}=\frac{E_c\ I_{tr,c}\ f_{ct}}{0.9\ E_{frp}\ t_{frp}}, \quad (2)$$

where E_c and E_{frp} are the moduli of elasticity of the concrete and the FRP respectively, $I_{tr,c}$ is the cracked second moment of area of the plated section transformed into equivalent concrete, f_{ct} the cylinder splitting tensile strength of concrete and t_{frp} the FRP plate thickness. If the splitting tensile strength is not determined from tests, f_{ct} (in MPa) is taken as $0.56\sqrt{f_c'}$ where f_c' is the concrete cylinder compressive strength.

The concrete shear strength V_c of the beam is calculated by Oehlers (1992) using the Australian code AS 3600 (Standards Australia, 1988) equation, given as:

$$V_c=\left[1.4-\left(d/2000\right)\right]bd\left(\rho_s f_c'\right)^{1/3}, \quad (3)$$

where b and d are the width and effective depth of the beam cross section, respectively; ρ_s is the ratio of tension steel reinforcement.

1.2. Jansze's model

Jansze (1997) proposed a plate-end debonding strength model, which was originally developed for steel-plated beams. The proposed model considered the occurrence of PE debonding failure at the onset of shear cracking in RC beams. The critical shear force at the plate end which causes debonding, $V_{db,end}$, is given as:

$$V_{db,end}=\tau_{PES}bd=0.18\sqrt[3]{3\frac{d}{a'}}\left(1+\sqrt{\frac{200}{d}}\right)\sqrt[3]{100\rho_s f_c'}bd, \quad (4)$$

where a' is a modified shear span, equal to:

$$a'=\sqrt[4]{\frac{\left(1-\sqrt{\rho_s}\right)^2}{\rho_s}dL_{up}{}^3}, \quad (5)$$

in which L_{up} is the unplated length. If a' is greater than the actual shear span, a, then the average value of both values $\left(a'+a\right)/2$ should be used.

1.3. Ahmed and van Germert's model

The Jansze's (1997) model was modified by Ahmed and van Germert (1999) to account for the difference between FRP and steel properties and also to include the effect of shear reinforcement. The modified equation proposed by Ahmed and van Germert (1999) is given:

$$V_{db,end}=\left(\tau_{PES}+\tau\Delta_{mod}\right)bd, \quad (6)$$

where

$$\tau\Delta_{mod}=\tau_{PES}bd\left(\frac{S_s}{I_{s,c}b_{frp}}-\frac{S_{frp}}{I_{frp,c}b_a}\right)+6188.5\left(\frac{\tau-4.121}{bd}\right); \quad (7)$$

$$\tau=\left(0.15776\sqrt{f_c'}+\frac{17.2336\rho_s d}{a}\right)+0.9\frac{A_{sv}f_{yv}}{sb}, \quad (8)$$

where τ_{PES} is the same as suggested by Jansze (1997) as per Eqn (4); S_{frp} and S_s are the first moments of area about the neural axis, respectively, for FRP plate, and that of an equivalent steel plate. The equivalent steel plate is the one that has the same tensile capacity and width as that of the FRP plate but with an equivalent thickness determined assuming that the yield stress of steel is 550 MPa. The terms $I_{frp,c}$ and $I_{s,c}$ are the moments of inertia of a cracked plated section with FRP plates and equivalent steel plates, respectively, while b_{frp} and b_a are the widths of FRP plate and adhesive, respectively, which can be practically considered the same. The terms A_{sv} and f_{yv} are the cross sectional area and yield stress of the steel stirrups, whereas s is the stirrup spacing.

1.4. Smith and Teng's model

Smith and Teng (2002b) proposed a model that is based on the concrete shear strength only. The debonding shear force at the plate end, $V_{db,end}$, is given by:

$$V_{db,end}=1.5V_c, \quad (9)$$

where V_c is the shear capacity of the concrete calculated based on the Australian code AS 3600 (Standards Australia, 1988) given by Eqn (3). The applicability of this model is suggested to be limited for FRP strengthened beams with the ratio of the applied moment to the ultimate moment $M_{db,end}/M_u\le 0.67$.

1.5. Colotti's et al. model

A theoretical model based on truss analogy was proposed by Colotti et al. (2004) to predict the failure mode and ultimate capacity of RC beams strengthened with FRP. In this model, the load capacity of the beam is predicted as the minimum value obtained from four different shear strength equations corresponding to: (a) plate-debonding failure; (b) shear failure; (c) tension/concrete crushing failure; and (d) rupture of FRP plates.

The ultimate shear load for the plate-end failure mode of FRP-strengthened beam is given by:

$$V_{db,end} = p_y d\left[\phi + \alpha - \sqrt{(\phi+\alpha)^2 - 2\phi\beta}\right], \quad p_y > 0, \qquad (10)$$

where p_y is the strength of the transverse reinforcement taken as $p_y = A_{sv} f_{yv}/s$; α is the ratio of shear span to beam effective depth, $\alpha = a/d$; β represents the ratio of plate length in shear to beam effective depth, $\beta = l_a/d$; and ϕ is the ratio of bond strength to stirrup strength, $\phi = U_y/p_y$.

Two equations to determine the limiting bond strength are provided in this model. They characterize the two types of PE debonding failure. The limiting bond strength in the case of PE interfacial debonding is given by:

$$U_y = b_m\left[2.77 + 0.06\left(f_c' - 20\right)\right] \text{ for } f_c' > 20\,\text{MPa}. \qquad (11)$$

The effective width of the plate-adhesive interface, b_m, is assumed to be the average of the beam and FRP plate widths: $b_m = \left(b + b_{frp}\right)/2$.

For the case of concrete cover separation, the effective bond strength is taken as the minimum value calculated by Eqn (11) above and Eqn (12) below:

$$U_y = \frac{f_{ct}\, s_c\, b}{C_c}, \qquad (12)$$

where f_{ct} is the tensile strength of the concrete; C_c is the concrete cover thickness (mm); s_c is the width of the tie element, assumed as a fraction of the crack spacing size l_c (mm) and taken as $s_c = l_c/5$. The crack spacing l_c could be calculated according to Eurocode 2 (European Committee for Standardization, 2004):

$$l_c = 50 + 0.25 k_1 k_2 \phi_s/\rho_r, \qquad (13)$$

where ϕ_s is the diameter of tension steel reinforcement; k_1 and k_2 are coefficients for crack spacing size taken as 0.8 and 0.5, respectively; and ρ_r is the effective tensile steel reinforcement ratio taken as $\rho_r = A_{se}/2.5bc_c$, in which the effective area of flexural tension reinforcement $A_{se} = A_s/2$.

Shear failure in the concrete web or yielding of the steel stirrups is assumed to occur when:

$$V = \frac{bdf_c}{2}\left[\sqrt{1+\alpha^2} - \alpha\right] + p_y d\alpha \text{ for}$$

$$0 \le \frac{p_y}{bf_c} \le \frac{\sqrt{1+\alpha^2} - \alpha}{2\sqrt{1+\alpha^2}}; \qquad (14a)$$

$$V = \sqrt{p_y b d^2 f_c\left(1 - \frac{p_y}{bf_c}\right)} \text{ for } \frac{\sqrt{1+\alpha^2} - \alpha}{2\sqrt{1+\alpha^2}} \le \frac{p_y}{bf_c} \le 0.5; \qquad (14b)$$

$$V = \frac{bdf_c}{2} \text{ for } \frac{p_y}{bf_c} > 0.5 \qquad (14c)$$

in which f_c is the effective concrete compressive strength. The failure of the concrete web or the failure of the longitudinal reinforcement occurs when the shearing force is:

$$V = p_y d\left[\sqrt{\frac{2T_y}{p_y d} + \alpha^2} - \alpha\right] \text{ for } \frac{p_y}{bf_c} > \frac{\sqrt{1+\alpha^2} - \alpha}{2\sqrt{1+\alpha^2}}; \qquad (15a)$$

$$V = \frac{bdf_c}{2}\left[\sqrt{\frac{4T_y}{bdf_c}\left(1 - \frac{T_y}{bdf_c}\right) + \alpha^2} - \alpha\right] \text{ for}$$

$$\frac{p_y}{bf_c} \le \frac{\sqrt{1+\alpha^2} - \alpha}{2\sqrt{1+\alpha^2}},\ T_y \le 0.5bdf_c; \qquad (15b)$$

$$V = \frac{bdf_c}{2}\left[\sqrt{1+\alpha^2} - \alpha\right] \text{ for } \frac{p_y}{bf_c} \le \frac{\sqrt{1+\alpha^2} - \alpha}{2\sqrt{1+\alpha^2}},$$

$$T_y > 0.5bdf_c. \qquad (15c)$$

Composite failure by rupture of FRP reinforcement, failure of main tensile steel or concrete crushing occurs when:

$$V = \frac{M_u}{a}, \qquad (16)$$

where the flexural capacity of the cross section is calculated as specified in ACI 440.R2 guide (ACI, 2002).

1.6. Teng and Yao's model

Yao and Teng (2007) and Teng and Yao (2007) conduced experimental and analytical investigations on FRP-strengthened beams which led to modify the moment-shear interaction expression proposed by Oehlers (1992). The modified interaction equation as proposed by Teng and Yao (2007) is as follows:

$$\left(\frac{M_{db,end}}{0.85M_{db,f}}\right)^2 + \left(\frac{V_{db,end}}{0.85V_{db,s}}\right)^2 = 1.0, \qquad (17)$$

where the flexural debonding moment $M_{db,f}$ of FRP plate end terminated in a pure bending region is given by:

$$M_{db,f} = \frac{0.488M_{u,0}}{\left(\alpha_{flex}\,\alpha_{axial}\,\alpha_w\right)^{1/9}} \le M_{u,0}, \qquad (18)$$

where $M_{u,0}$ is the moment capacity of the unplated section; α_{flex}, α_{axial} and α_w are three dimensionless parameters reflecting the effect of the contribution of the FRP to the flexural rigidity of the cracked section, the effect of the axial rigidity ratio, and the effect of the width ratio, respectively, defined by:

$$\alpha_{flex} = \frac{(EI)_{c,frp} - (EI)_{c,0}}{(EI)_{c,0}},\ \alpha_{axial} = \frac{E_{frp}\, t_{frp}}{E_c\, d},$$

$$\alpha_w = \frac{b}{b_{frp}} \le 3, \qquad (19)$$

where $(EI)_{c,frp}$ and $(EI)_{c,0}$ are the flexural rigidities of the cracked section with and without FRP, respectively; E_{frp} and t_{frp} are the modulus of elasticity and thickness of FRP plates.

The shear debonding force $V_{db,s}$ at an FRP plate end terminated at or near the supports was modified by Teng and Yao (2007). In addition to V_c component, the contributions of FRP plate V_{frp}, and internal shear steel reinforcement $\varepsilon_{v,e}\overline{V_s}$ to the shear capacity of the beam were also added as follows:

$$V_{db,s} = V_c + V_{frp} + \varepsilon_{v,e}\overline{V_s}, \tag{20}$$

where $\overline{V_s}$ is the shear force carried by the shear steel reinforcement per unit strain, given by:

$$\overline{V_s} = A_{sv}E_{sv}d/s \tag{21}$$

in which E_{sv} is the elastic modulus of the stirrups. In Eqn (20), $\varepsilon_{v,e}$ is the effective strain in the stirrups. The best-fit expression for $\varepsilon_{v,e}$ is given by:

$$\varepsilon_{v,e} = \frac{10}{\left(\alpha_{flex}\,\alpha_E\,\alpha_t\,\alpha_w\right)^{1/2}}, \tag{22}$$

where α_E represents the elastic moduli ratio $\alpha_E = E_{frp}/E_c$; and α_t is the ratio between the FRP plate thickness and the effective depth of the section $\alpha_t = \left(t_{frp}/d\right)^{1.3}$.

For the predictions of the shear capacity contributed by the concrete V_c and the FRP plate V_{frp}, Teng and Yao (2007) suggested that Oehlers et al.'s prestress model (Oehlers et al., 2004, 2005) is to be adopted. For design purposes, however, Teng and Yao (2007) explained that the shear capacity of concrete beams, V_c, to be used in Eqn (20) can be obtained from current code specified equations, while the contribution of V_{frp} is usually small enough and could be ignored.

1.7. *fib* Bulletin 14 model

The *fib* Bulletin 14 (*fib*, 2001) presented the model proposed by Blaschko (1997) which is based on the concrete shear strength of the beam. This model indicates that PE debonding may be prevented by limiting the acting shear force at the plate end to the shear cracking strength of the beam as follows:

$$V_{db,end} < 0.15 f_{ck}^{1/3}\, bd, \tag{23}$$

where f_{ck} is the characteristic compressive strength of concrete determined according to Eurocode 2 (European Committee for Standardization, 2004).

1.8. Concrete Society TR 55 model

The Technical Report 55 (TR55) of the Concrete Society (2012) recommended an upper limit for the acting shear force at the plate end region to avoid PE debonding:

$$V_{db,end} < 0.67 V_{Rd}, \tag{24}$$

where V_{Rd} is the shear strength of the beam section determined in accordance with Section 6.2 of Eurocode 2 (European Committee for Standardization, 2004).

1.9. ACI 440.2R model

The ACI 440 Committee in its document ACI 440.2R (ACI, 2017) provides also an upper limit for the factored shear force at the termination point of the plate to avoid PE debonding:

$$V_{db,end} < 0.67 V_c, \tag{25}$$

where V_c is the concrete shear strength of the beam section determined in accordance with the ACI 318 code (ACI, 2014).

1.10. AS 5100.8 model

The Australian Standard AS 5100.8 (Standards Australia, 2017b) follows similar approach to that of TR 55 of Concrete Society (2012) and ACI 440.2R (ACI, 2017) by prescribing an upper limit for the acting shear force at the plate end region:

$$V_{db,end} < 0.67 V_u, \tag{26}$$

where V_u is the nominal shear strength of the beam section determined in accordance with the AS 5100.5 standard (Standards Australia, 2017a).

2. Experimental database of PE debonding failure

A relatively large database including 128 beam test results from 32 different studies was established, as given in Table 1. The beams included in the database were collected based on the following criteria: (1) all beams failed by PE debonding either by interfacial debonding or CCS; (2) all beams were simply supported and were tested under one- or two-point loading systems; (3) the FRP plate/sheet was neither prestressed nor anchored at its ends; and (4) sufficient details for various geometric and material parameters were provided. The database had a broad range of design parameters. Considering the beam geometry, the width of the test beams was in the range of 100 to 400 mm with a total beam height of 100 to 450 mm, while the clear span ranged from 812 to 3800 mm. The test beams had different shear span/depth ratio in the range of 2.29 to 6.25. The tension steel reinforcement ratio ranged from 0.32 to 2.12%. Considering the material type, the database included 43 beams strengthened by pultruded FRP plates and 85 beams strengthened by wet lay-up FRP sheets. The width of the FRP was in the range 30 to 360 mm. The thickness of a single layer of dry fibers was in the range of 0.11 to 0.176 mm for the wet lay-up FRP sheets while the total thickness for pultruded FRP was in the range of 0.82 to 4.76 mm. The elastic modulus of the FRP materials ranged between 10.3 and 400 GPa. The ratio of the plated length beyond the point load to the shear span of the beam was in the range of 0.25–1.00. The compressive strength of the beams was in the range of 19.2 to 66.4 MPa. A total of 114 beams were tested under two-point loading system while 14 beams were tested under one-point loading system. Table 1 gives relevant details for the beams included in this database.

Table 1. Database of beams failed by plate-end debonding

Ref.	No.	Beam	RC beam			Steel reinforcement				FRP reinforcement				Loading configuration			$P_{u,exp}$ (kN)
			b (mm)	d (mm)	f'_c (MPa)	Ten. Rein	f_y (MPa)	f_{yv} (MPa)	ρ_{sv}	E_{frp} (GPa)	f_{fu} (MPa)	t_{frp} (mm)	b_{frp} (mm)	L (mm)	a (mm)	L_{up} (mm)	
Ritchie et al. (1991)	1	C	152	250.8	40.0	2-12.7	414	250	0.0064	11.72	160.6	4.76	152.0	2,438	914	8.0	110.8
	2	D	152	250.8	40.0	2-12.7	414	250	0.0064	11.72	160.6	4.76	151.1	2,438	914	8.0	119.3
	3	G	152	250.8	43.3	2-12.7	414	250	0.0064	10.3	184.1	4.19	152.0	2,438	914	0.0	125.8
	4	I	152	250.8	40.0	2-12.7	414	250	0.0064	27.579	319.2	4.06	149.9	2,438	914	8.0	101.2
	5	M	152	250.8	43.3	2-12.7	414	250	0.0064	117.9	1,489.2	1.27	152.0	2,438	914	0.0	144.1
Quantrill et al. (1996)	6	B2	100	84	42.4	3-6	350	350	0.0028	49.00	1,078	1×1.2	80.0	900	300	20.0	34.0
	7	B3	100	84	42.4	3-6	350	350	0.0028	49.00	1,078	1×1.2	30.0	900	300	20.0	24.6
	8	B4	100	84	42.4	3-6	350	350	0.0028	49.00	1,078	1×1.6	60.0	900	300	20.0	35.0
	9	B6	100	84	42.4	3-6	350	350	0.0028	118.50	987	1×1.2	80.0	900	300	20.0	40.8
Arduini et al. (1997)	10	A4	200	163	33.0	2-14	540	540	0.0019	167.00	2,906	1×1.3	150.0	2,000	700	150.0	110.0
	11	A5	200	163	33.0	2-14	540	540	0.0019	167.00	2,906	2×1.3	150.0	2,000	700	150.0	90.0
	12	B3	200	163	33.0	3-13	540	540	0.0034	400.00	3,000	3×0.17	300.0	2,500	1,100	100.0	228.0
Garden et al. (1997)	13	1Bu	100	68	47.3	3-6	350	350	0.0028	111.11	1,273	1×0.7	65.0	900	300	20.0	36.6
	14	2Bu	100	68	47.3	3-6	350	350	0.0028	111.11	1,273	1×0.7	65.0	900	340	20.0	34.0
	15	3Bu	100	68	47.3	3-6	350	350	0.0028	111.11	1,273	1×0.7	65.0	900	400	20.0	34.6
	16	1Cu	100	68	47.3	3-6	350	350	0.0028	111.11	1,273	1×1.0	45.0	900	300	20.0	32.0
	17	2Cu	100	68	47.3	3-6	350	350	0.0028	111.11	1,273	1×1.0	45.0	900	340	20.0	35.6
	18	3Cu	100	68	47.3	3-6	350	350	0.0028	111.11	1,273	1×1.0	45.0	900	400	20.0	30.8
Garden et al. (1998)	19	B1u ,1.0	100	84	43.2	3-6	350	350	0.0028	111.00	1,414	0.82	67.0	900	300	20.0	32.0
	20	B3u ,1.0	100	84	43.2	3-6	350	350	0.0028	111.00	1,414	0.82	67.0	900	340	20.0	34.0
	21	B4u ,1.0	100	84	43.2	3-6	350	350	0.0028	111.00	1,414	0.82	67.0	900	400	20.0	34.5
	22	B1u ,2.3	130	206	37.6	3-10	556	556	0.0029	115.00	1,284	1.28	90.0	2,200	845	40.0	100.3
Beber et al. (1999)	23	VR5	120	214	33.6	2-10	565	738	0.0043	230.00	3,400	4×0.11	120.0	2,350	783	75.0	102.2
	24	VR6	120	214	33.6	2-10	565	738	0.0043	230.00	3,400	4×0.11	120.0	2,350	783	75.0	100.6
	25	VR7	120	214	33.6	2-10	565	738	0.0043	230.00	3,400	7×0.11	120.0	2,350	783	75.0	124.2
	26	VR8	120	214	33.6	2-10	565	738	0.0043	230.00	3,400	7×0.11	120.0	2,350	783	75.0	124.0
David et al. (1999)	27	P2	150	257	40.0	2-14	500	500	0.0027	150.00	2,400	1×1.2	100.0	2,800	933	200.0	136.0
	28	P3	150	257	40.0	2-14	500	500	0.0027	150.00	2,400	1×1.2	100.0	2,800	933	200.0	142.2
	29	P4	150	257	40.0	2-14	500	500	0.0027	150.00	2,400	2×1.2	100.0	2,800	933	200.0	156.0
	30	P5	150	257	40.0	2-14	500	500	0.0027	150.00	2,400	2×1.2	100.0	2,800	933	200.0	159.0
Hau et al. (1999)	31	2	150	205	35.4	2-10	537	537	0.0105	19.72	259	1.32	150.0	1,500	500	350.0	106.0
Tumialan et al. (1999)	32	A3	150	250	51.7	4-15.9	427	427	0.0076	230.0	3,400	3×0.165	150.0	2,130	1,065	0.0	172.2
	33	A8	150	250	51.7	4-15.9	427	427	0.0076	230.0	3,400	6×0.165	75.0	2,130	1,065	0.0	196.4
	34	C2	150	250	51.7	4-15.9	427	427	0.0038	230.0	3,400	3×0.165	150.0	2,130	1,065	0.0	158.6
Ahmed (2000)	35	AF.2	125	193	41	2-8	568	553	0.0064	240	3,500	2×0.167	75	1,500	500	200	83.0
	36	AF.2.1	125	193	41	2-8	568	553	0.0064	240	3,500	2×0.167	75	1,500	500	150	85.8
	37	AF.3	125	193	41	2-8	568	553	0.0064	240	3,500	2×0.167	75	1,500	500	100	96.6
	38	AF.4	125	193	41	2-8	568	553	0.0064	240	3,500	2×0.167	75	1,500	500	50	111.0
	39	BF.2-1	125	193	41	2-8	568	553	0.0027	240	3,500	2×0.167	75	1,500	500	50	90.0
	40	BF.3-1	125	193	41	2-8	568	553	0.0045	240	3,500	2×0.167	75	1,500	500	50	104.0
	41	CF.2-1	125	193	43	2-8	568	553	0.0064	240	3,500	2×0.167	75	1,500	500	100	104.8
	42	CF.3-1	125	193	43	3-8	568	553	0.0064	240	3,500	2×0.167	75	1,500	500	100	118.2
	43	CF.4-1	125	193	43	2-10	568	553	0.0064	240	3,500	2×0.167	75	1,500	500	100	140.2
	44	DF2	125	193	42	3-8	568	553	0.0045	240	3,500	2×0.167	75	1,500	500	50	120.5
	45	DF3	125	193	40.5	3-8	568	553	0.0045	240	3,500	2×0.167	75	1,500	500	50	120.0
	46	DF4	125	193	40.5	3-8	568	553	0.0045	240	3,500	2×0.167	75	1,500	500	50	125.5
	47	EF.1-1	125	193	46	3-8	568	553	0.0045	240	3,500	2×0.167	75	1,500	500	50	131.8
	48	EF.3-1	125	193	38	3-8	568	553	0.0045	240	3,500	2×0.167	75	1,500	500	50	119.0
	49	EF.4-1	125	193	33	3-8	568	553	0.0045	240	3,500	2×0.167	75	1,500	500	50	120.6
Matthys (2000)	50	BF2	200	409	36.5	4-16	590	560	0.0050	159	3,200	1×1.2	100	3,800	1250	70	370.0
	51	BF3	200	409	34.9	4-16	590	560	0.0050	159	3,200	1×1.2	100	3,800	1250	70	372.0
	52	BF4	200	409	30.8	4-16	590	560	0.0050	159	3,200	1×1.2	100	3,800	1250	70	368.4
	53	BF5	200	409	37.4	4-16	590	560	0.0050	159	3,200	1×1.2	100	3,800	1250	70	354.0
Fanning and Kelly (2001)	54	F5	155	203	66.4	3-12	532	305.5	0.0029	155	2,400	1×1.2	120	2,800	1100	385	100.0
	55	F6	155	203	66.4	3-12	532	305.5	0.0029	155	2,400	1×1.2	120	2,800	1100	385	103.0
	56	F7	155	203	66.4	3-12	532	305.5	0.0029	155	2,400	1×1.2	120	2,800	1100	462	97.5
	57	F10	155	203	66.4	3-12	532	305.5	0.0029	155	2,400	1×1.2	120	2,800	1100	550	82.0
Gao et al. (2001)	58	1N4	150	162	35.7	2-10	460	460	0.0089	235	4,200	4×0.11	75	1,500	500	150	86.4
	59	1N6	150	162	35.7	2-10	460	460	0.0089	235	4,200	6×0.110	75	1,500	500	150	86.3
Maalej and Bian (2001)	60	Beam3	115	125	30.3	3-10	534	365	0.0082	230	3,400	0.111	115	1,350	500	75	86.0
	61	Beam4	115	125	30.3	3-10	534	365	0.0082	230	3,400	0.111	115	1,350	500	75	82.0
	62	Beam5	115	125	30.3	3-10	534	365	0.0082	230	3,400	0.111	115	1,350	500	75	79.0
Nguyen et al. (2001)	63	A950	120	120	25.7	3-10	384	400	0.0094	181	3,140	1×1.2	80	1,330	440	190	56.2
	64	A1100	120	120	25.7	3-10	384	400	0.0094	181	3,140	1×1.2	80	1,330	440	115	57.4
	65	A1150	120	120	25.7	3-10	384	400	0.0094	181	3,140	1×1.2	80	1,330	440	90	59.0

End of Table 1

Ref.	No.	Beam	RC beam			Steel reinforcement				FRP reinforcement				Loading configuration			$P_{u,exp}$ (kN)
			b (mm)	d (mm)	f'_c (MPa)	Ten. Rein	f_y (MPa)	f_{yv} (MPa)	ρ_{sv}	E_{frp} (GPa)	f_{fu} (MPa)	t_{frp} (mm)	b_{frp} (mm)	L (mm)	a (mm)	L_{up} (mm)	
Rahimi and Hutchinson (2001)	66	A4	200	120	49.2	2-10	575	575	0.0019	127	1,532	1×0.2	150	2,100	750	85	61.9
	67	A6	200	120	49.2	2-10	575	575	0.0019	127	1,532	1×0.2	150	2,100	750	85	59.4
	68	A8	200	120	49.2	2-10	575	575	0.0019	127	1,532	1×0.2	150	2,100	750	85	65.2
	69	B5	200	120	49.2	2-10	575	575	0.0038	127	1,532	1×0.2	150	2,100	750	85	69.7
Smith and Teng (2003)	70	1A	154	215	31.5	2×10	506	506	0.0102	271	3,720	2×0.165	147	1,500	500	250	59.7
	71	1B	154	215	31.5	2×10	506	506	0.0102	271	3,720	2×0.165	147	1,500	500	25	100.2
	72	2A	151	215	48.6	2×10	506	506	0.0095	271	3,720	2×0.165	147	1,500	500	375	48.1
	73	2B	151	215	48.6	2×10	506	506	0.0095	271	3,720	2×0.165	147	1,500	500	125	86.4
	74	3A	151	215	45.3	2×10	506	506	0.0095	257	4,519	2×0.165	147	1,500	500	175	79.9
	75	3B	151	215	45.3	2×10	506	506	0.0095	257	4,519	2×0.165	147	1,500	500	50	98.0
Valcuende et al. (2003)	76	A-S1	100	128	39.5	2×10	500	500	0.0057	165	2,600	1×1.2	50	1,000	400	50	78.6
	77	B-S1	100	128	41.6	2×10	500	500	0.0057	165	2,600	1×1.2	50	1,000	400	50	70.2
Breña and Macri (2004)	78	A1-I	102	89	42.2	1×9.5	435	420	0.0053	230	3,790	1×0.165	51	812	330	25	27.9
	79	A2-I	102	89	42.2	1×9.5	435	420	0.0053	230	3,790	2×0.165	51	812	330	25	31.4
	80	A3-I	102	89	53.3	1×9.5	435	420	0.0053	230	3,790	3×0.165	51	812	330	25	39.0
	81	A4-I	102	89	53.3	1×9.5	435	420	0.0053	230	3,790	2×0.165	76	812	330	25	36.8
	82	A5-I	102	89	53.3	1×9.5	435	420	0.0053	230	3,790	1×0.165	102	812	330	25	35.2
	83	A1-II	102	89	42.2	2×9.5	435	420	0.0053	230	3,790	1×0.165	51	812	330	25	40.2
	84	A2-II	102	89	42.2	2×9.5	435	420	0.0053	230	3,790	2×0.165	51	812	330	25	44.5
	85	A3-II	102	89	53.3	2×9.5	435	420	0.0053	230	3,790	3×0.165	51	812	330	25	48.0
	86	A4-II	102	89	53.3	2×9.5	435	420	0.0053	230	3,790	2×0.165	76	812	330	25	52.5
	87	A5-II	102	89	53.3	2×9.5	435	420	0.0053	230	3,790	1×0.165	102	812	330	25	48.9
Gao et al. (2004a)	88	1T6LN	150	162	47.8	2×10	460	250	0.0089	235	4,200	6×0.11	150	1,500	500	20	116.2
	89	2T6LN	150	162	62.1	2×10	460	250	0.0089	235	4,200	6×0.11	150	1,500	500	20	135.9
	90	2T4LN	150	162	62.1	2×10	460	250	0.0089	235	4,200	4×0.11	150	1,500	500	20	133.3
Gao et al. (2004b)	91	A0	150	162	35.7	2×10	531	250	0.0089	235	4,200	2×0.11	75	1,500	500	150	80.7
	92	B0	150	162	35.7	2×10	531	250	0.0089	235	4,200	4×0.11	75	1,500	500	150	86.4
Grace and Singh (2005)	93	Bb1	152	211.2	31.0	3×15.9	414	414	0.0091	138	2,070	1×1.2	152	2,540	864	152.5	136.6
	94	Bb3	152	211.2	31.0	3×15.9	414	414	0.0091	227	2,758	2×0.2	152	2,540	864	152.5	133.5
Pham and Al-Mahaidi (2006)	95	E1a	140	220	53.7	3×12	551	334	0.0090	209	3,900	6×0.176	100	2,300	700	150	141.4
	96	E1b	140	220	53.7	3×12	551	334	0.0090	209	3,900	6×0.176	100	2,300	700	150	149.2
	97	E2a	140	220	53.7	3×12	551	334	0.0090	209	3,900	6×0.176	100	2,300	700	350	102.8
	98	E2b	140	220	53.7	3×12	551	334	0.0090	209	3,900	6×0.176	100	2,300	700	350	106.8
	99	E3a	140	220	53.7	2×12	551	334	0.0090	209	3,900	6×0.176	100	2,300	700	150	132.0
	100	E3b	140	220	53.7	2×12	551	334	0.0090	209	3,900	6×0.176	100	2,300	700	150	130.4
	101	E4a	140	220	53.7	3×12	551	334	0.0090	209	3,900	6×0.176	100	2,300	700	150	158.0
	102	E4b	140	220	53.7	3×12	551	334	0.0090	209	3,900	6×0.176	100	2,300	700	150	122.4
	103	E5a	140	220	53.7	3×12	551	334	0.0090	209	3,900	9×0.176	100	2,300	700	150	126.6
	104	E5b	140	220	53.7	3×12	551	334	0.0090	209	3,900	9×0.176	100	2,300	700	150	126.4
	105	E3b2	140	220	53.7	3×12	551	334	0.0090	209	3,900	6×0.176	100	1,600	700	150	120.0
Benjeddou et al. (2007)	106	RB1	120	129	21.0	2×10	400	235	0.0047	165	2,800	1×1.2	100	1,800	600	50	40.1
Esfahani et al. (2007)	107	B3-12D-2L15	150	166	25.2	2×12	400	350	0.0084	240	3,800	2×0.176	150	1,600	600	100	70.9
	108	B4-12D-3L15	150	166	25.2	2×12	400	350	0.0084	240	3,800	3×0.176	150	1,600	600	100	74.4
Yao and Teng (2007)	109	CS-B	150	215	24.6	2×10	536	536	0.0105	256	4,114	2×0.165	148	1,500	500	50	81.5
	110	CS-L3-B	150	215	26.3	2×10	536	536	0.0105	256	4,114	3×0.165	148	1,500	500	50	78.5
	111	CS-W100-B	150	215	30.2	2×10	536	536	0.0105	256	4,114	2×0.165	100	1,500	500	50	80.9
	112	CP-B	150	215	29.6	2×10	536	536	0.0105	165	2,800	1×1.2	148	1,500	500	50	76.1
Ceroni (2010)	113	A3	100	150	26.9	2×10	452	537	0.0067	230	3,450	2×0.167	100	2,000	880	300	40.0
	114	B2	100	150	26.9	2×12	441	537	0.0067	230	3,450	1×0.167	100	1,800	780	400	49.2
	115	B3	100	150	26.9	2×12	441	537	0.0067	230	3,450	2×0.167	100	1,800	780	400	48.2
Al-Tamimi et al. (2011)	116	B85P	110	155	50.0	2×10	611	420	0.0114	215	2,500	1×1.4	100	1,690	561.5	84.5	60.7
	117	B70P	110	155	50.0	2×10	611	420	0.0114	215	2,500	1×1.4	100	1,690	561.5	169	47.1
	118	B25P	110	155	50.0	2×10	611	420	0.0114	215	2,500	1×1.4	100	1,690	561.5	422.5	51.9
Sadrmomtazi et al. (2014)	119	C2	100	130	40.0	2×10	382	379	0.0168	235	3,900	2×0.111	100	1,000	333	50	75.8
Al-Saawani et al. (2015)	120	S-0.5-35-360	400	215	35.0	3×14	470	420	0.0038	165	2,800	1×1.4	360	3,000	1000	100	235.1
Hasnat et al. (2016)	121	S(AT1)C	150	166	48.3	2×8	414	414	0.0118	120	2,260	1×1.2	100	1,296	432	50	100.0
	122	B(AT1)C	150	166	47.5	2×8	414	414	0.0118	120	2,260	1×1.2	100	1,296	432	50	101.6
Skuturna and Valivonis (2016)	123	BC1-1	100	175	28.0	2×8	562	358	0.0113	232	3,850	1×0.167	100	1,200	400	50	79.0
	124	BC1-2	100	175	28.0	2×8	562	358	0.0113	232	3,850	1×0.167	100	1,200	400	50	78.0
	125	BC2-1	100	175	28.0	2×8	562	358	0.0113	232	3,850	1×0.167	100	1,200	400	50	79.5
	126	BC3-1	100	175	19.2	2×8	562	358	0.0113	232	3,850	1×0.167	100	1,200	400	50	68.0
	127	BC4-1	100	175	26.4	2×6	358	358	0.0057	232	3,850	1×0.167	100	1,200	400	50	44.0
	128	BC4-2	100	175	26.4	2×6	358	358	0.0057	232	3,850	1×0.167	100	1,200	400	50	48.0

3. Proposed method for predicting PE debonding capacity

Previous studies (Oehlers, 1992; Smith & Teng, 2002a; Zhang & Teng, 2016; Achintha & Burgoyne, 2008, 2011) indicated that there is a relationship between the PE debonding failure and the shear cracks developed at the plate end region in FRP strengthened RC beams. This explains the existence of several shear based models that were developed for predicting PE debonding failure as reviewed in the preceding section. The goal of this study is to develop a simple model capable of predicting the PE debonding failure of FRP strengthened RC beams. The proposed model is to be expressed as a function of the concrete shear strength V_c of the beam as follows:

$$V_{db,end} = \beta V_c. \tag{27}$$

The equation developed by Zsutty (1971) for evaluating V_c was selected to be used in this proposed model. It is given as follows:

$$V_c = 2.17\left(f_c'\rho_s\frac{d}{a}\right)^{1/3} bd, \tag{28}$$

where f_c' is the specified concrete compressive strength of the beam; ρ_s is the longitudinal reinforcement ratio of the main steel; d is the effective depth of the beam; and a is the shear span. The Zsutty's equation was decided to be used in this model because it accounts for the main design parameters known to affect V_c and gives accurate and reliable predictions for the concrete shear strength of RC beams (Zsutty, 1971).

The term β in Eqn (27) is a factor that will be determined. It can be noted that the proposed model is similar to the model of Smith and Teng (2002b) (Eqn (9)) and to that of the ACI 440.2R (ACI, 2017) (Eqn (25)). In Smith and Teng's model (2002b), the factor β was 1.5 whereas in the ACI 440.2R (ACI, 2017) model, the factor β was 0.67. The actual variation of the factor β can be determined using the experimental database given in Table 1. The ratio of the experimental shear force V_{exp}, corresponding to the PE debonding failure, to the calculated concrete shear strength of the beams V_c was plotted against V_c as shown in Figure 3. The V_c values of the beams were calculated using Eqn (28). Figure 3 indicates that almost all beams gave a ratio of V_{exp}/V_c higher than 1, meaning that all the beams failed after the onset of the major shear crack. The range of the ratio V_{exp}/V_c was between 0.98 and 2.91. The figure also indicates that the factor β of 0.67 proposed by ACI 440.2R (ACI, 2017) is very conservative. On the other hand, the factor β of 1.5 proposed by Smith and Teng (2002b) seems to be better than that of the ACI 440.2R (ACI, 2017). However, having a fixed value for the factor β does not seem appropriate as the beams of the database showed a relatively large band width of variation of the ratio V_{exp}/V_c. Instead, the parameters that control the widening of the shear cracks should be considered in formulating the factor β. This is because the widening of the shear cracks at the plate end region is responsible for triggering the PE debonding failure as previously discussed. The amount of the shear reinforcement is one of the main parameters that control the opening of the shear cracks. Also, the amount of the longitudinal reinforcement has an influence on the opening of the shear cracks. The influences of these parameters are discussed in the following subsections.

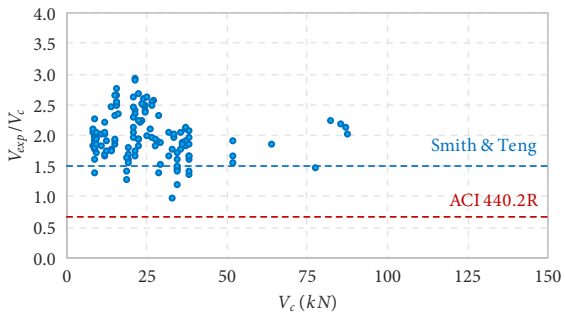

Figure 3. Variation of the ratio V_{exp}/V_c for PE debonding database

3.1. Influence of longitudinal reinforcement ratio

It was established that the amount of main tensile reinforcement has a beneficial effect on increasing the concrete shear strength V_c and limiting the widening of the shear crack in RC beams (Kani, 1999; Rebeiz, 1999). This effect was recognized by most of the design methods by incorporating the longitudinal reinforcement ratio ρ_s of the main steel in their V_c design equations. Eqn (28) includes ρ_s among the main parameters that contribute to V_c. Recently, El-Sayed (2014) has indicated that external FRP longitudinal strengthening also contributes to the concrete shear strength of RC beams. Its effect has been considered by replacing the effective depth and steel reinforcement ratio in V_c design equations by the equivalent effective depth d_{eq} and equivalent reinforcement ratio ρ_{eq} as follows:

$$d_{eq} = \frac{A_s E_s d + A_{frp} E_{frp} h}{A_s E_s + A_{frp} E_{frp}}; \tag{29}$$

$$\rho_{eq} = \frac{\left(A_s + A_{frp}\dfrac{E_{frp}}{E_s}\right)}{\left(bd_{eq}\right)}, \tag{30}$$

where A_s and E_s are the internal steel area and modulus of elasticity; A_{frp} and E_{frp} are the external FRP area and modulus of elasticity; b, d and h are beam width, effective depth of tension steel, and total depth of beam, respectively. Thus, the influence of the longitudinal reinforcement is not included in formulating the factor β as it is already considered in the V_c equation.

3.2.Influence of shear reinforcement ratio

In the light of understanding the mechanism of PE debonding, it is anticipated that the reinforcing stirrups will have a beneficial effect on the PE debonding capacity

of FRP strengthened beams. The reinforcing stirrups control the opening of the shear crack and also increase the resistance to the bond failure of concrete splitting along the main longitudinal steel. To the best knowledge of the authors, no systematic study has been conducted to investigate the influence of reinforcing stirrups on the PE debonding failure. Among the beams tested by Ahmed (2000), there were 3 beams with different amounts of steel stirrups. The results indicated that the PE debonding failure load increased with the increase of the stirrup amount. To quantify the effect of the stirrup reinforcement ratio ρ_v, the experimental shear strength corresponding to the PE debonding failure of the beams included in the database was plotted against ρ_v. To eliminate the effect of the location of the cut-off point of FRP along the shear span, the beams with FRP reinforcement extended to the support (within 50 mm from the support) were only considered. Figure 4 shows a plot of the experimental shear strength V_{exp} normalized with respect to the calculated V_c against ρ_v for 62 test beams from the database with FRP terminated at the supports. It should be pointed out that the calculated concrete shear strength V_c of the beams was calculated using Eqn (28) after replacing d and ρ_s by d_{eq} and ρ_{eq}, respectively. Figure 4 indicates that the PE debonding capacity increases with the increase of the shear reinforcement ratio ρ_v. It was found that the shear strength at PE debonding failure is proportional to $(\rho_v)^{0.06}$. Based on this analysis, the factor β_v that can be introduced into Eqn (27) to account for the influence of the shear reinforcement can be expressed as:

$$\beta_v = 2.15(\rho_v)^{0.06}. \tag{31}$$

It can be noted that the factor β_v is a function of the amount of shear reinforcement ratio only and does not include the effect of the grade of the steel stirrups. This is because PE debonding generally occurs after the formation of the shear cracks but before the occurrence of the shear failure of the beam.

3.3. Influence of the location of FRP cut-off point

Several studies indicated that PE debonding failure is related to the shear force and bending moment in the beam at the FRP plate end (Oehlers, 1992; Yao & Teng, 2007; Teng & Yao, 2007; Ahmed, 2000; Matthys, 2000; Fanning & Kelly, 2001; Nguyen et al., 2001; Smith & Teng, 2003; Pham & Al-Mahaidi, 2006). Experimental results obtained from those studies indicated that the PE debonding failure load decreased with the increase of the plate end distance from the support in simply supported beams. This is because in the case of beams with FRP terminated at the supports, the shear force is the highest while the bending moment is zero at the plate end region. On the other hand, when the FRP plate end is moved away from the support, the bending moment increases relative to the shear force at the plate end region leading to the reduction of the PE debonding failure load. To account for this effect in the proposed model, a factor β_L can be introduced into

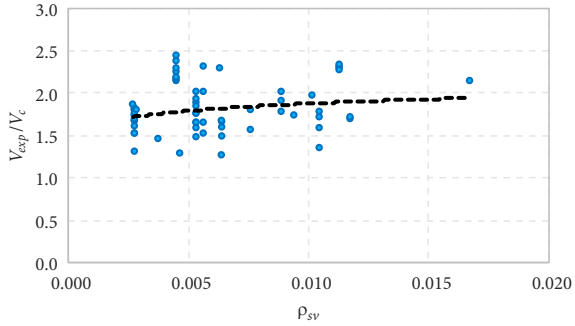

Figure 4. Influence of shear reinforcement ratio on PE debonding capacity

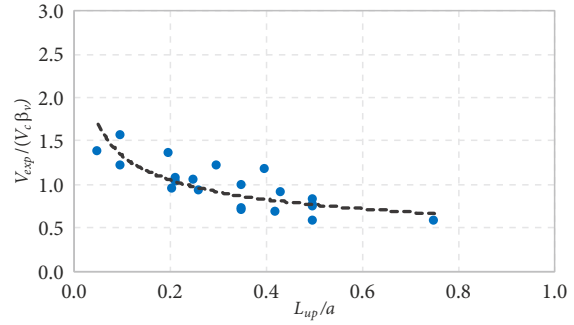

Figure 5. Influence of the location of FRP cut-off point on PE debonding capacity

Eqn (27). This factor represents the ratio of the unplated length L_{up} along the beam (measured from the support to the plate end) to the shear span a. The factor β_L can be obtained by plotting the experimental shear strength of selected beams in the database against the ratio L_{up}/a as presented in Figure 5. Twenty-one data points were used for generating Figure 5. These data were selected from five different studies (Ahmed, 2000; Fanning & Kelly, 2001; Nguyen et al., 2001; Smith & Teng, 2003; Pham & Al-Mahaidi, 2006) where the unplated length was varied. The vertical axis of the figure represents the experimental shear strength V_{exp} normalized with respect to the calculated V_c and the factor β_v, while the horizontal axis represents the ratio L_{up}/a. The figure shows the decrease of the normalized shear force with the increase of the ratio L_{up}/a. This correlation resulted in the factor β_L, which can be expressed as:

$$\beta_L = 0.57\left(\frac{L_{up}}{a}\right)^{-0.34} \le 1.0. \tag{32}$$

It can be noted that an upper limit of 1.0 was set for the factor β_L indicating that when the FRP is extended to the support, β_L equals 1.0. This value is reduced to reach 0.57 when $L_{up} = a$.

3.4. Proposed equation

Based on the previous analysis and discussion, the proposed shear force at the plate end corresponding to the PE debonding failure can be expressed as:

$$V_{db,end} = \beta_v \beta_L 2.17 \left(f_c' \rho_{eq} \frac{d_{eq}}{a} \right)^{1/3} b d_{eq}, \quad (33)$$

where the factors β_v and β_L are as given in Eqns (31) and (32), respectively. Also, the equivalent effective depth d_{eq} and equivalent reinforcement ratio ρ_{eq} are as given in Eqns (29) and (30), respectively. It can be noted that the shear span, a, can be determined in the case of a beam under concentrated loading as it is the distance from the concentrated load to the support. For a beam with uniformly distributed loading, the term a in Eqn (33) can be replaced by the ratio of the factored moment to the factored shear, M/V, occur simultaneously at the critical section for shear. On the other hand, for calculating the factor β_L as per Eqn (32) for a beam under uniformly distributed loading, the term a can be replaced by $L/2$, where L is the span of the beam.

4. Verification of the proposed equation

To verify the proposed method, Eqn (33) was used for calculating the shear force V_{cal} at the FRP plate end for 128 beams included in the collected database. The calculations of Eqn (33) were compared with the experimental shear force V_{exp} of the beams. Table 2 gives the ratio of V_{exp}/V_{cal} for each beam. The table also gives the average ratio of V_{exp}/V_{cal}, the coefficient of variation, and the percentage of specimens with unconservative predictions expressed as the exceedance percentage for the 128 beams. The exceedance percentage is defined as the percentage of number of tests with V_{cal} exceeding V_{exp} meaning that the ratio of V_{exp}/V_{cal} is less than 1.0. Table 2 shows that the proposed equation gave reasonably accurate and conservative predictions with an average ratio of V_{exp}/V_{cal} of 1.14 for the 128 beams included in the database. The table also shows that the proposed method gave reasonably scattered predictions with a coefficient of variation of 17.7% and percentage of exceedance of 20.3%. Figure 6 shows the variation of the ratio V_{exp}/V_{cal} against the parameters f_c', ρ_{eq}, ρ_v, and L_{up}/a which are known to affect the PE debonding capacity. The figure shows that the ratio V_{exp}/V_{cal} varied consistently over a relatively smaller band width of the scattered results. This can be observed for the variation of V_{exp}/V_{cal} against each of the four variables shown in the figure.

5. Comparison with existing shear based models

To further verify the proposed equation, the predictions of Eqn (33) were compared with those from the existing shear based models presented earlier in the paper. The same 128 test data were used in this comparison. The predictions for each beam using the ten shear based models are also given in Table 2. Figure 7 compares the predictions of the proposed equation with the predictions of these methods. It can be observed from Table 2 and Figure 7 that *fib* Bulletin 14 (*fib*, 2001), ACI 440.2R (ACI, 2017), and Oheler (1992) gave very conservative predictions compared to the proposed equation. The average ratio of V_{exp}/V_{cal} for these methods were 3.87, 2.78, and 1.7, respectively, compared to 1.14 for the proposed equation.

Table 2. Comparison of experimental results with predictions of PE debonding failure load

No.	V_{exp} (kN)	Experimental to calculated shear load at failure, V_{exp}/V_{cal}													
			Shear capacity based models										Other code predictions		
		Proposed model	Oehler (1992)	Jansze (1997)	Ahmed and Van Germert (1999)	Smith and Teng (2002b)	Colotti et al. (2004)	Teng and Yao (2007)	*fib* Bulletin 14 (2001) Eqn (23)	TR55 (2012) Eqn (24)	ACI 440.2R (2017)	AS 5100.8 (2017)	*fib* Bulletin 14 (2001) Eqn (34)	TR55 (2012) Eqn (37)	CNR-DT 200 (2013)
1	55.4	0.93	1.16	0.63	0.63	1.18	0.61	0.84	2.83	0.89	2.03	0.90	1.35	1.46	1.33
2	59.6	1.00	1.25	0.67	0.67	1.27	0.65	0.90	3.05	0.95	2.18	0.97	1.46	1.57	1.43
3	62.9	1.05	1.26	0.41	0.41	1.31	0.66	0.84	3.13	1.00	2.21	1.02	1.58	1.69	1.55
4	50.6	0.80	1.06	0.57	0.57	1.08	0.55	0.88	2.59	0.81	1.85	0.82	1.10	1.20	1.07
5	72.0	1.06	1.45	0.47	0.47	1.50	0.76	1.22	3.59	1.14	2.54	1.16	1.45	1.64	1.40
6	17.0	1.12	1.60	0.88	0.88	1.32	1.04	1.01	3.87	1.68	2.74	1.51	1.11	1.24	1.11
7	12.3	0.86	1.16	0.64	0.64	0.95	0.90	0.75	2.80	1.21	1.98	1.10	1.07	1.15	1.12
8	17.5	1.15	1.66	0.91	0.90	1.36	1.14	1.06	3.98	1.72	2.82	1.56	1.17	1.30	1.22
9	20.4	1.19	1.96	1.06	1.05	1.58	1.25	1.19	4.64	2.01	3.29	1.82	1.06	1.21	1.06
10	55.0	1.06	1.73	1.39	1.39	1.26	1.06	1.35	3.51	1.41	2.59	1.32	1.21	1.50	1.17
11	45.0	0.76	1.51	1.14	1.14	1.03	0.86	1.08	2.87	1.16	2.12	1.08	0.95	1.19	0.92
12	114.0	0.76	1.01	1.20	1.19	1.20	0.59	1.07	2.26	0.83	1.69	0.91	1.20	1.36	1.11
13	18.3	1.15	1.65	0.92	0.91	1.37	1.14	1.04	4.02	1.79	2.80	1.61	1.17	1.30	1.14
14	17.0	1.11	1.53	0.85	0.85	1.27	0.98	1.00	3.73	1.66	2.60	1.49	1.23	1.37	1.20
15	17.3	1.20	1.56	0.87	0.86	1.29	0.92	1.08	3.80	1.69	2.64	1.52	1.47	1.64	1.44
16	16.0	1.01	1.46	0.80	0.80	1.20	1.06	0.93	3.51	1.56	2.44	1.41	1.07	1.18	1.08
17	17.8	1.17	1.62	0.89	0.89	1.33	1.11	1.07	3.91	1.74	2.72	1.56	1.35	1.49	1.36
18	15.4	1.07	1.40	0.77	0.77	1.15	0.89	0.98	3.38	1.50	2.35	1.35	1.37	1.52	1.39
19	16.0	1.02	1.51	0.82	0.82	1.23	1.02	0.95	3.62	1.58	2.56	1.43	0.99	1.11	1.02
20	17.0	1.13	1.61	0.88	0.87	1.31	1.01	1.05	3.85	1.68	2.72	1.52	1.19	1.34	1.22
21	17.3	1.21	1.63	0.89	0.89	1.33	0.94	1.12	3.90	1.71	2.76	1.54	1.42	1.60	1.46
22	50.2	1.19	1.57	1.10	1.10	1.39	0.96	1.44	3.73	1.54	2.69	1.47	1.26	1.42	1.27
23	51.1	1.32	1.79	1.65	1.65	1.74	0.79	1.48	4.11	0.73	3.03	0.76	1.46	1.76	1.38
24	50.3	1.30	1.76	1.63	1.62	1.71	0.78	1.46	4.05	0.71	2.98	0.75	1.44	1.73	1.36
25	62.1	1.48	2.21	2.01	2.00	2.11	0.96	1.91	5.00	0.88	3.68	0.92	1.78	2.23	1.56

Continue of Table 2

No.	V_{exp} (kN)	Experimental to calculated shear load at failure, V_{exp}/V_{cal}													
			Shear capacity based models										Other code predictions		
		Proposed model	Oehler (1992)	Jansze (1997)	Ahmed and Van Germert (1999)	Smith and Teng (2002b)	Colotti et al. (2004)	Teng and Yao (2007)	*fib* Bulletin 14 (2001) Eqn (23)	TR55 (2012) Eqn (24)	ACI 440.2R (2017)	AS 5100.8 (2017)	*fib* Bulletin 14 (2001) Eqn (34)	TR55 (2012) Eqn (37)	CNR-DT 200 (2013)
26	62.0	1.48	2.21	2.00	2.00	2.11	0.96	1.90	4.99	0.88	3.68	0.92	1.78	2.22	1.56
27	68.0	1.11	1.55	1.57	1.57	1.35	1.06	1.44	3.44	1.21	2.46	1.19	1.22	1.50	1.23
28	71.1	1.17	1.62	1.65	1.64	1.41	1.10	1.50	3.60	1.26	2.57	1.25	1.28	1.56	1.29
29	78.0	1.17	1.89	1.80	1.80	1.55	1.21	1.69	3.94	1.38	2.82	1.37	1.48	1.86	1.52
30	79.5	1.19	1.92	1.84	1.84	1.58	1.23	1.73	4.02	1.41	2.88	1.40	1.51	1.90	1.55
31	53.0	1.21	1.16	1.83	1.93	1.57	1.09	1.37	3.50	0.38	2.56	0.41	0.92	1.14	0.90
32	86.1	0.98	1.25	0.33	0.33	1.16	1.30	0.94	4.11	0.80	2.82	0.75	1.00	1.04	0.96
33	98.2	1.12	1.26	0.38	0.38	1.33	1.48	1.34	4.69	0.91	3.21	0.86	1.17	1.25	1.17
34	79.3	0.95	1.06	0.30	0.30	1.07	1.28	1.06	3.78	1.24	2.59	1.08	0.92	0.95	0.89
35	41.5	1.39	1.71	1.89	2.00	1.59	1.13	1.41	3.33	0.57	2.37	0.61	1.23	1.34	1.22
36	42.9	1.30	1.61	1.87	1.92	1.64	0.99	1.29	3.44	0.59	2.45	0.63	1.27	1.38	1.26
37	48.3	1.28	1.83	1.97	1.96	1.85	0.96	1.30	3.87	0.66	2.76	0.71	1.43	1.56	1.42
38	55.5	1.45	1.48	1.90	1.89	2.12	0.97	1.37	4.45	0.76	3.17	0.81	1.65	1.79	1.63
39	45.0	1.24	1.55	1.54	1.54	1.72	1.03	1.23	3.61	1.18	2.57	1.26	1.34	1.45	1.32
40	52.0	1.38	1.55	1.78	1.78	1.99	0.99	1.35	4.17	0.94	2.97	1.00	1.54	1.68	1.53
41	52.4	1.29	1.69	1.89	1.88	1.81	1.02	1.28	4.13	0.71	2.92	0.75	1.33	1.43	1.32
42	59.1	1.40	1.87	1.99	1.99	1.94	1.15	1.38	4.66	0.81	3.30	0.84	1.35	1.44	1.34
43	70.1	1.53	1.52	2.07	2.06	2.07	1.40	1.51	5.53	0.96	3.91	0.98	1.29	1.36	1.29
44	60.3	1.44	1.75	1.72	1.72	1.99	1.13	1.45	4.79	1.08	3.40	1.12	1.39	1.47	1.38
45	60.0	1.40	1.77	1.74	1.73	2.01	1.15	1.55	4.83	1.08	3.45	1.12	1.31	1.55	1.30
46	62.8	1.41	1.99	1.82	1.81	2.10	1.20	1.65	5.05	1.13	3.61	1.17	1.35	1.69	1.32
47	65.9	1.53	2.33	1.83	1.82	2.12	1.19	1.52	5.08	1.18	3.55	1.22	1.50	1.59	1.48
48	59.5	1.48	1.99	1.76	1.76	2.04	1.17	1.50	4.89	1.08	3.53	1.12	1.39	1.47	1.38
49	60.3	1.57	2.04	1.87	1.86	2.16	1.26	1.63	5.20	1.10	3.84	1.15	1.44	1.54	1.43
50	185.0	1.30	2.15	1.44	1.44	1.77	1.34	1.67	4.55	0.90	3.30	0.93	1.23	1.53	1.33
51	186.0	1.32	2.08	1.47	1.47	1.81	1.37	1.71	4.64	0.91	3.40	0.93	1.25	1.56	1.37
52	184.2	1.37	2.07	1.52	1.52	1.87	1.44	1.79	4.79	0.91	3.58	0.93	1.30	1.61	1.42
53	177.0	1.23	2.25	1.37	1.37	1.68	1.27	1.58	4.31	0.86	3.12	0.88	1.16	1.45	1.26
54	50.0	1.02	1.91	1.24	1.24	0.91	1.09	1.21	2.62	1.30	1.72	1.16	1.09	1.34	1.06
55	51.5	1.05	1.97	1.28	1.28	0.94	1.12	1.25	2.69	1.34	1.77	1.20	1.12	1.38	1.10
56	48.8	1.05	2.07	1.27	1.27	0.89	1.20	1.28	2.55	1.26	1.68	1.13	1.06	1.31	1.04
57	41.0	0.94	1.81	1.09	1.11	0.75	1.19	1.17	2.15	1.06	1.41	0.95	0.89	1.10	0.87
58	43.2	1.24	1.22	1.67	1.67	1.46	1.05	1.30	3.60	0.55	2.63	0.54	1.26	1.36	1.31
59	43.2	1.18	1.25	1.67	1.67	1.46	1.05	1.39	3.60	0.55	2.62	0.54	1.16	1.32	1.22
60	43.0	1.60	1.23	1.68	1.67	1.88	1.57	1.36	6.40	1.15	4.79	1.11	1.28	1.35	1.24
61	41.0	1.49	1.08	1.60	1.59	1.80	1.50	1.47	6.10	1.10	4.57	1.06	1.17	1.41	1.13
62	39.5	1.39	1.70	1.54	1.53	1.73	1.45	1.51	5.88	1.06	4.40	1.02	1.16	1.43	1.05
63	28.1	1.27	1.77	1.46	1.44	1.30	1.71	1.48	4.41	0.62	3.40	0.61	0.90	1.08	0.95
64	28.7	1.09	2.83	1.31	1.30	1.32	1.33	1.31	4.50	0.63	3.47	0.63	0.92	1.11	0.97
65	29.5	1.03	2.73	1.27	1.26	1.36	1.26	1.30	4.63	0.65	3.57	0.64	0.94	1.14	1.00
66	31.0	0.88	2.66	0.94	0.94	0.94	0.51	0.89	2.35	0.99	1.62	0.97	1.24	1.46	1.15
67	29.7	0.79	2.54	0.90	0.90	0.90	0.49	0.87	2.25	0.95	1.56	0.93	1.13	1.41	1.00
68	32.6	0.93	2.35	0.99	0.99	0.99	0.54	0.94	2.47	1.04	1.71	1.02	1.31	1.54	1.21
69	34.9	0.89	2.33	1.06	1.05	1.05	0.49	1.00	2.64	0.70	1.83	0.71	1.32	1.65	1.17
70	39.8	1.00	1.22	1.41	1.53	1.17	0.87	1.02	2.54	0.29	1.89	0.31	0.72	0.79	0.68
71	66.8	1.21	1.83	1.45	1.44	1.96	0.73	1.10	4.26	0.48	3.17	0.52	1.21	1.33	1.14
72	32.1	0.82	0.84	1.07	1.19	0.83	1.22	0.99	1.80	0.25	1.25	0.27	0.54	0.60	0.50
73	57.6	1.01	1.36	1.62	1.63	1.48	0.69	0.97	3.24	0.45	2.25	0.48	0.97	1.07	0.90
74	53.3	1.08	1.33	1.61	1.68	1.40	0.77	1.02	3.07	0.41	2.15	0.44	0.92	1.01	0.85
75	65.3	1.08	1.54	1.51	1.50	1.72	0.66	0.97	3.76	0.51	2.64	0.54	1.13	1.24	1.05
76	39.3	1.46	2.65	1.61	1.60	1.95	1.44	1.71	6.01	1.22	4.31	1.19	1.19	1.42	1.29
77	35.1	1.29	2.31	1.42	1.41	1.71	1.26	1.49	5.28	1.08	3.75	1.06	1.05	1.25	1.13
78	14.0	0.95	1.22	0.79	0.79	1.09	0.67	0.75	2.94	0.73	2.09	0.73	1.15	1.24	1.16
79	15.7	1.02	1.40	0.89	0.89	1.23	0.75	0.93	3.31	0.82	2.35	0.82	1.14	1.25	1.16
80	19.5	1.12	1.57	1.03	1.02	1.42	0.83	1.05	3.81	1.00	2.60	0.99	1.24	1.38	1.25
81	18.4	1.06	1.46	0.97	0.96	1.34	0.70	0.96	3.59	0.94	2.45	0.94	1.13	1.26	1.07
82	17.6	1.06	1.37	0.93	0.92	1.28	0.61	0.84	3.44	0.90	2.34	0.90	1.15	1.27	1.05
83	20.1	1.12	1.74	0.85	0.85	1.25	0.96	0.93	4.24	1.05	3.01	0.97	1.07	1.12	1.08
84	22.3	1.21	1.96	0.94	0.94	1.39	1.06	1.15	4.70	1.16	3.33	1.08	1.10	1.16	1.11
85	24.0	1.17	1.90	0.94	0.93	1.38	1.02	1.14	4.69	1.23	3.20	1.13	1.07	1.15	1.07
86	26.3	1.28	2.05	1.03	1.02	1.51	1.00	1.20	5.13	1.34	3.50	1.24	1.14	1.23	1.10
87	24.5	1.23	1.88	0.96	0.95	1.41	0.85	1.00	4.77	1.25	3.26	1.15	1.11	1.18	1.05
88	58.1	1.11	1.77	1.24	1.23	1.79	0.80	1.23	4.39	1.12	3.05	1.15	1.17	1.42	1.06
89	68.0	1.19	1.82	1.33	1.32	1.92	0.84	1.27	4.71	1.28	3.13	1.31	1.30	1.54	1.16
90	66.7	1.25	1.77	1.30	1.30	1.88	0.83	1.19	4.62	1.26	3.07	1.28	1.42	1.59	1.27
91	40.4	1.23	1.51	1.56	1.56	1.37	1.10	0.97	3.36	0.80	2.45	0.82	1.19	1.25	1.19
92	43.2	1.24	1.70	1.67	1.67	1.46	1.18	1.24	3.60	0.85	2.63	0.88	1.15	1.24	1.16
93	68.3	1.05	2.05	1.35	1.35	1.32	1.48	1.29	4.52	0.67	3.37	0.66	1.02	1.23	1.01
94	66.8	1.07	1.95	1.32	1.32	1.29	1.44	1.01	4.41	0.65	3.30	0.64	1.05	1.10	1.02
95	70.7	1.04	1.72	1.51	1.51	1.41	1.21	1.24	4.06	0.85	2.76	0.84	0.99	1.24	0.90
96	74.6	1.10	1.82	1.59	1.59	1.49	1.27	1.30	4.28	0.90	2.92	0.89	1.05	1.31	0.95

End of Table 2

No.	V_{exp} (kN)	Experimental to calculated shear load at failure, V_{exp}/V_{cal}													
			Shear capacity based models										Other code predictions		
		Proposed model	Oehler (1992)	Jansze (1997)	Ahmed and Van Germert (1999)	Smith and Teng (2002b)	Colotti et al. (2004)	Teng and Yao (2007)	*fib* Bulletin 14 (2001) Eqn (23)	TR55 (2012) Eqn (24)	ACI 440.2R (2017)	AS 5100.8 (2017)	*fib* Bulletin 14 (2001) Eqn (34)	TR55 (2012) Eqn (37)	CNR-DT 200 (2013)
97	51.4	1.01	1.40	1.30	1.35	1.03	1.42	1.07	2.95	0.62	2.01	0.61	0.72	0.90	0.65
98	53.4	1.05	1.45	1.35	1.41	1.07	1.48	1.12	3.06	0.64	2.09	0.64	0.75	0.94	0.68
99	66.0	1.05	1.64	1.67	1.67	1.51	0.89	1.29	3.79	0.79	2.58	0.81	1.17	1.46	1.06
100	65.2	1.04	1.62	1.65	1.65	1.49	0.88	1.27	3.74	0.78	2.55	0.81	1.15	1.45	1.05
101	79.0	1.16	1.93	1.69	1.68	1.58	1.35	1.38	4.53	0.95	3.09	0.94	1.11	1.39	1.01
102	61.2	0.90	1.49	1.31	1.30	1.22	1.04	1.07	3.51	0.74	2.39	0.73	0.86	1.07	0.78
103	63.3	0.88	1.59	1.35	1.35	1.27	1.08	1.16	3.63	0.76	2.47	0.76	0.93	1.17	0.84
104	63.2	0.88	1.59	1.35	1.35	1.26	1.08	1.15	3.63	0.76	2.47	0.75	0.93	1.17	0.84
105	67.5	1.08	1.68	1.71	1.71	1.54	0.91	1.32	3.87	0.81	2.64	0.83	1.19	1.50	1.08
106	20.1	0.83	1.55	0.91	0.91	1.08	0.72	1.10	3.13	1.08	2.49	1.02	0.98	1.20	0.98
107	35.5	0.90	1.51	1.18	1.18	1.18	0.69	0.95	3.24	0.56	2.50	0.57	0.98	1.07	0.94
108	37.2	0.90	1.61	1.24	1.24	1.24	0.72	1.09	3.40	0.59	2.63	0.60	0.96	1.10	0.91
109	54.3	1.09	1.75	1.54	1.54	1.76	0.71	1.03	3.86	0.38	3.00	0.40	1.01	1.18	0.96
110	52.3	0.97	1.64	1.45	1.45	1.66	0.66	1.08	3.63	0.36	2.79	0.39	0.92	1.15	0.84
111	53.9	1.05	1.57	1.43	1.42	1.63	0.74	0.94	3.58	0.37	2.68	0.40	1.07	1.15	1.05
112	50.7	0.83	1.51	1.35	1.35	1.55	0.61	1.07	3.39	0.35	2.55	0.37	0.85	1.06	0.82
113	20.0	1.16	1.52	1.34	1.33	1.02	0.82	1.21	2.97	0.44	2.27	0.45	1.27	1.36	1.22
114	24.6	1.49	1.76	1.50	1.50	1.11	1.57	1.13	3.65	0.54	2.79	0.54	1.23	1.28	1.20
115	24.1	1.40	1.86	1.47	1.47	1.09	1.54	1.35	3.58	0.53	2.73	0.53	1.12	1.18	1.09
116	30.4	0.74	1.41	1.12	1.11	1.16	0.59	0.98	3.22	0.45	2.22	0.46	0.84	1.05	0.78
117	23.5	0.67	1.21	1.03	1.02	0.90	0.56	0.86	2.50	0.35	1.72	0.36	0.65	0.82	0.61
118	26.0	1.00	1.72	1.32	1.42	0.99	1.82	1.53	2.76	0.38	1.90	0.39	0.78	0.97	0.68
119	37.9	1.28	2.37	1.53	1.52	1.85	1.18	0.92	5.68	0.58	4.06	0.59	1.14	1.23	1.07
120	117.5	0.89	1.27	1.27	1.27	1.23	0.57	1.24	2.79	0.85	2.04	0.88	1.40	1.75	1.33
121	50.0	1.03	1.54	1.59	1.58	1.75	0.72	1.15	3.68	0.50	2.55	0.53	1.29	1.48	1.30
122	50.8	1.05	1.58	1.62	1.62	1.79	0.74	1.18	3.76	0.51	2.61	0.54	1.32	1.51	1.33
123	39.5	1.42	2.18	1.85	1.84	2.11	0.97	0.89	4.96	0.67	3.76	0.71	1.22	1.30	1.17
124	39.0	1.40	2.16	1.82	1.81	2.08	0.96	0.88	4.89	0.66	3.72	0.70	1.20	1.28	1.15
125	39.8	1.42	2.20	1.86	1.85	2.12	0.98	0.89	4.99	0.68	3.79	0.72	1.23	1.31	1.18
126	34.0	1.38	2.27	1.80	1.79	2.06	0.97	0.87	4.84	0.59	3.91	0.62	1.11	1.18	1.08
127	22.0	0.96	1.26	1.34	1.33	1.45	0.67	0.83	2.81	0.67	2.16	0.72	1.18	1.34	1.10
128	24.0	1.05	1.38	1.46	1.45	1.58	0.74	0.91	3.07	0.73	2.36	0.79	1.29	1.46	1.20
Average =		1.14	1.70	1.33	1.33	1.47	1.01	1.20	3.87	0.93	2.78	0.91	1.17	1.35	1.15
C.V. =		17.7%	22.6%	30.5%	30.6%	23.9%	28.2%	21.4%	23.1%	40.6%	24.4%	36.2%	18.1%	18.6%	19.1%
Exceedance =		20.3%	0.8%	25.0%	25.0%	8.6%	49.2%	26.6%	0.0%	62.5%	0.0%	62.5%	21.1%	5.5%	21.9%

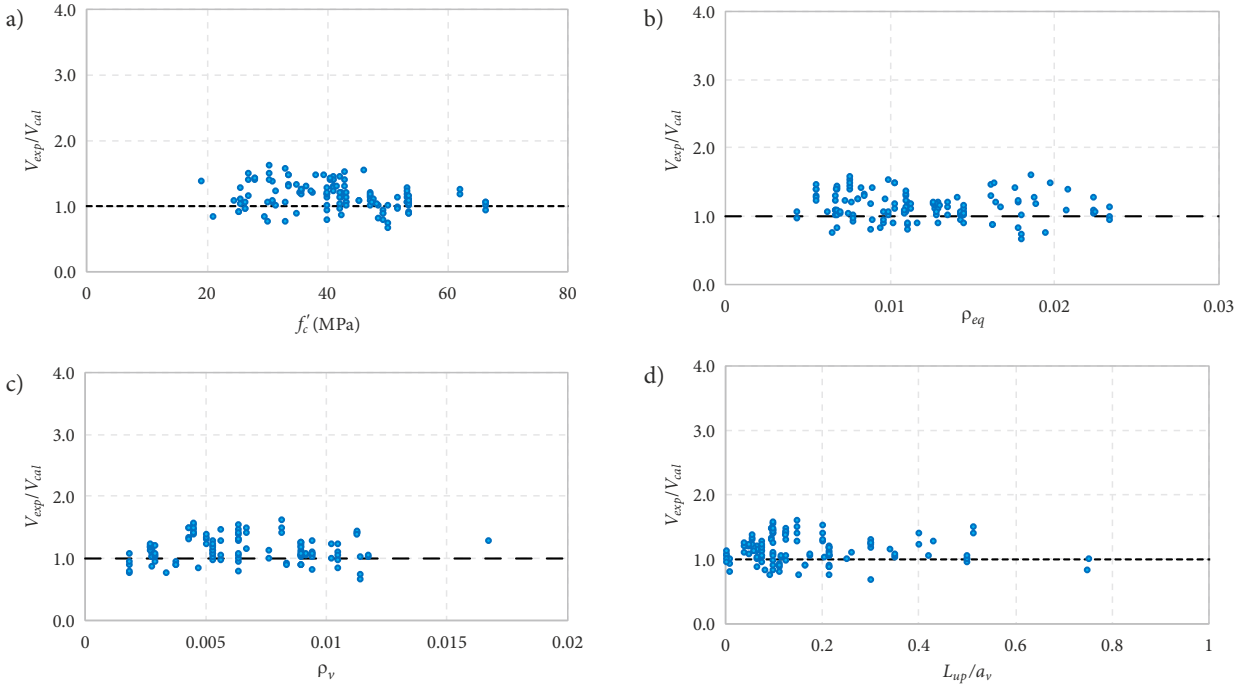

Figure 6. Experimental to predicted shear force by proposed equation at PE debonding versus: a – concrete compressive strength; b – equivalent longitudinal reinforcement ratio; c – shear reinforcement ratio; d – unplated length to shear span ratio

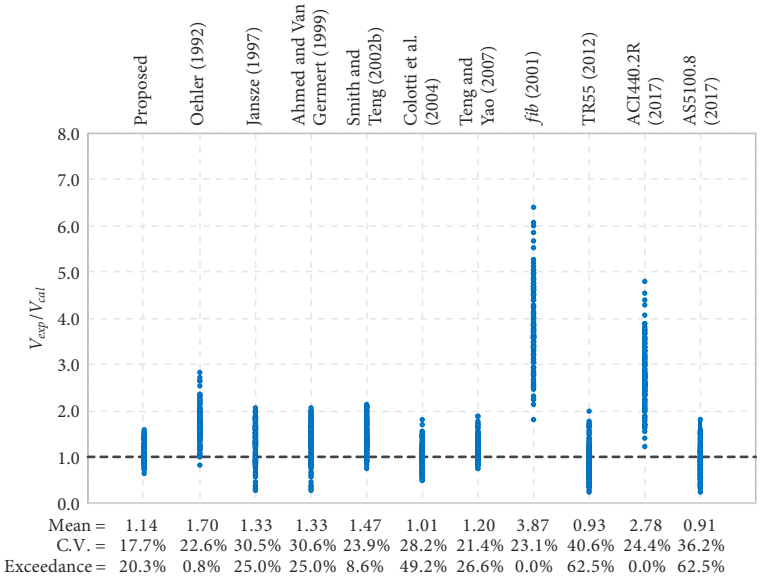

Figure 7. Comparison of predictions of the proposed equation with the existing shear based models

The corresponding coefficients of variation for these methods were 23.1%, 24.4%, and 22.6% which are higher than 17.7% of the proposed equation. Table 2 and Figure 7 also show that the models of Jansze (1997), Ahmed and Van Germert (1999), and Smith and Teng (2002b) gave conservative predictions with average ratios of V_{exp}/V_{cal} of 1.33, 1.33, and 1.47, respectively. These levels of conservatism are less than those of the preceding three models but still more conservative than that obtained by the proposed method. These three methods also showed more scatter predictions which were reflected by the relatively higher coefficients of variation of 30.5%, 30.6%, and 23.9%, respectively. On the other hand, both TR55 of Concrete Society (2012) and Australian Standard AS 5100.8 (Standards Australia, 2017b) provided unconservative predictions with average ratios of V_{exp}/V_{cal} of 0.93 and 0.91, respectively. The two methods provided unconservative predictions for 62.5% of the beams in the database as can be noticed from Table 2 and Figure 7. Although the model of Colotti et al. (2004) gave an average ratio of V_{exp}/V_{cal} of 1.01, it showed inconsistent predictions with coefficient of variation of 28.2% and unconservative predictions for 49.2% of the beams in the database. Table 2 and Figure 7 indicate that the model of Teng and Yao (2007) provided reasonably accurate and conservative predictions close to those of the proposed equation. The average ratio of V_{exp}/V_{cal} for this model was 1.2 compared to 1.14 for the proposed equation. However, the coefficient of variation and the percentage of exceedance for this model were 21.4% and 26.6% compared to 17.7% and 20.3%, respectively for the proposed equation.

The conducted comparison with the shear based models indicates that the proposed equation provided better predictions in terms of accuracy and consistency. Moreover, the proposed equation has the advantage of being much simpler than most of these existing models.

6. Comparison with other code provisions

In this section, the proposed equation is to be further verified by comparison with other existing code models that are based on different approaches rather than shear strength. In this comparison, the models of *fib* Bulletin 14 (*fib*, 2001), TR55 of Concrete Society (2012), and Italian code CNR-DT 200 (National Research Council, 2013) are used. These models restrict the tensile strain in the FRP at ultimate limit state to the debonding strain ε_{fd}. The debonding strain is used to calculate the moment capacity of FRP strengthened RC section. Different equations for determining ε_{fd} are recommended by the different codes and guidelines. The *fib* Bulletin 14 (*fib*, 2001) gives the following equations for calculating ε_{df} on the basis of fracture mechanics approach:

$$\varepsilon_{fd}=\begin{cases}\alpha_1 c_1 k_c k_b\sqrt{f_{ct}/n_{frp}E_{frp}t_{frp}} & , \ l_b \geq l_{b,\max}\\ \alpha_1 c_1 k_c k_b\sqrt{f_{ct}/n_{frp}E_{frp}t_{frp}}\cdot\left(l_b/l_{b,\max}\right)\left(2-l_b/l_{b,\max}\right), & l_b < l_{b,\max}\end{cases}, \tag{34}$$

where the maximum anchorage length $l_{b,\max}$ is given as follows:

$$l_{b,\max}=\sqrt{\left(n_{frp}E_{frp}t_{frp}\right)/\left(c_2 f_{ct}\right)}, \tag{35}$$

where α_1 is a reduction factor generally taken 0.9 but for beams with sufficient shear reinforcement and in slabs, it is taken 1.0; c_1 and c_2 are factors that can be taken 0.64 and 2.0, respectively for CFRP strips; f_{ct} is the tensile strength of concrete; n_{frp} is the number of FRP layers; k_c is a factor accounting for concrete compaction, generally taken 1.0 but for concrete with low compaction it is taken 0.67; k_b is a geometry factor given by:

$$k_b=1.06\sqrt{\left(2-b_{frp}/b\right)/\left(1+b_{frp}/400\right)}\geq 1, \ \text{with}$$
$$b_{frp}/b\geq 0.33. \tag{36}$$

The technical report TR55 of the Concrete Society (2012) recommends a similar equation to that of *fib* Bulletin 14 (*fib*, 2001) for determining ε_{fd}:

$$\varepsilon_{fd} = \begin{cases} 0.5k_b\sqrt{f_{ct}/n_{frp}E_{frp}t_{frp}} & , \ l_b \geq l_{b,\max} \\ 0.5k_b\sqrt{f_{ct}/n_{frp}E_{frp}t_{frp}}\left(l_b/l_{b,\max}\right)\left(2-l_b/l_{b,\max}\right) & , \ l_b < l_{b,\max} \end{cases}, \quad (37)$$

where k_b is a geometry factor taken as per Eqn (36) whereas the maximum anchorage length $l_{b,max}$ is given by:

$$l_{b,\max} = 0.7\sqrt{n_{frp}E_{frp}t_{frp}/f_{ct}}\ . \quad (38)$$

The Italian code CNR-DT 200 (National Research Council, 2013) also specifies an equation for calculating ε_{fd} based on fracture mechanics approach:

$$\varepsilon_{fd} = \begin{cases} 1/\gamma_{f,d}\sqrt{2\Gamma_{Fd}/n_{frp}E_{frp}t_{frp}} & , \ l_b \geq l_{b,\max} \\ 1/\gamma_{f,d}\sqrt{2\Gamma_{Fd}/n_{frp}E_{frp}t_{frp}}.\left(l_b/l_{b,\max}\right)\left(2-l_b/l_{b,\max}\right) & , \ l_b < l_{b,\max} \end{cases}, \quad (39)$$

where γ_{fd} is a safety factor and Γ_{Fd} is the design value of the specific fracture energy of the FRP-concrete interface given by:

$$\Gamma_{Fd} = k_b k_G\sqrt{f_c' f_{ct}}\ , \quad (40)$$

where f_c' and f_{ct} are the mean values of the concrete compressive and tensile strengths, respectively; k_G is a corrective factor taken for pre-cured FRP as 0.063 mm for the mean value and 0.023 mm for the 5% fractile value and taken for wet lay-up FRP as 0.077 mm for the mean value and 0.037 mm for the 5% fractile value; k_b is the geometrical corrective factor which is defined with the following equation:

$$k_b = \begin{cases} \sqrt{\left(2-b_{frp}/b\right)/\left(1+b_{frp}/b\right)} \geq 1, & b_{frp}/b \geq 0.25 \\ 1.18 & , \ b_{frp}/b < 0.25 \end{cases}. \quad (41)$$

The maximum anchorage length $l_{b,\max}$ is calculated by:

$$l_{b,max} = \min\left\{\left(1/\gamma_{Rd}f_{bd}\right)\sqrt{\pi^2\ E_{frp}t_{frp}\ \Gamma_{Fd}/2}, 200\ \text{mm}\right\} \quad (42)$$

in which

$$f_{bd} = \frac{2\ \Gamma_{Fd}}{S_u}, \quad (43)$$

with s_u = 0.25 mm is the design bond strength between FRP and concrete; and γ_{Rd} = 1.25 is a corrective factor.

The above equations for the three codes and guidelines were used for calculating the debonding strain ε_{fd} for each beam in the database, then the bending moment and shear force corresponding to PE debonding was obtained. Table 2 also compares the experimental shear force with the calculated shear force for each beam using the three methods. Figure 8 presents the comparison of the predictions of the proposed equation with those of the three code equations. It can be noticed that the proposed equation gave approximately comparable predictions to those of *fib* Bulletin 14 (*fib*, 2001) and Italian code CNR-DT 200 (National Research Council, 2013). The two methods gave average values of V_{exp}/V_{cal} of 1.17 and 1.15, respectively, with coefficients of variation of 18.1% and 19.1%. The corresponding values for the proposed method were 1.14 and 17.7%. Also, the exceedance percentage for *fib* Bulletin 14 (*fib*, 2001) and Italian code CNR-DT 200 (National Research Council, 2013) were 21.1% and 21.9% compared to 20.3% for the proposed equation. On the other hand, the Technical report TR55 of Concrete Society (2012) provided more conservative predictions with an average value of V_{exp}/V_{cal} of 1.35 with a coefficient of variation of 18.6% and an exceedance percentage of 5.5%.

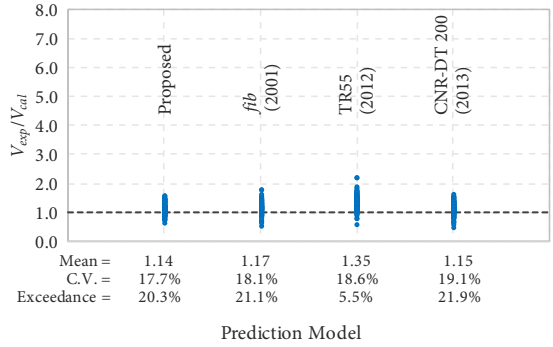

Figure 8. Comparison of predictions of the proposed equation with the other code models

This comparison indicates that the proposed equation presented conservative and accurate predictions similar to the best predictions from other code provisions that are based on fracture energy approach. Additionally, the proposed equation is still simpler than these of the existing provisions.

7. Prediction of governing debonding failure mode

As stated earlier in this paper, the two common debonding failure modes in FRP strengthened RC beams are IC debonding and PE debonding. For an FRP strengthened beam, it is important for the designer to be aware about the expected debonding failure mode. This is to be certain that the debonding capacity of the beam is greater than the factored design load. It is also important in the case of designing an anchorage system for the purpose of mitigating the premature debonding failure. FRP strengthened beams with relatively small shear span to depth ratio are prone to fail by PE debonding. While FRP strengthened beams with relatively high shear span to depth ratio are prone to fail by IC debonding. There is a transition zone in between for beams with intermediate shear span to depth ratio where the occurrence of any of the debonding failure modes is imminent. FRP external reinforcement is generally anchored at its ends for mitigating PE debonding in RC beams. On the other hand, anchorage of FRP reinforcement is applied at the midspan region for mitigating IC debonding in RC simply supported beams.

For beams in the transition zone where the PE and IC debonding capacities of the beam are close to each other, the critical regions at the FRP plate ends and midspan of the beam are required to be anchored. To come up with such a decision, the load carrying capacity of the beam corresponding to each debonding failure mode should be reliably determined.

For this purpose, the proposed equation for PE debonding could be combined with a reliable equation for predicting IC debonding of FRP strengthened beams. The two equations can be used to predict the debonding capacity of the beam and the expected debonding failure mode, either PE or IC debonding. The lesser value resulted from the two equations represents the debonding capacity of the beam and the corresponding type of failure (PE or IC debonding). The ACI 440.2R (ACI, 2017) method was proven to provide reliable predictions for IC debonding (Alfano et al., 2012) and therefore, it was selected to be used in this study. In this method, a design equation for determining the IC debonding strain ε_{fd} is recommended to be as follows:

$$\varepsilon_{fd} = 0.41\sqrt{\frac{f_c^{'}}{n_{frp}E_{frp}t_{frp}}} \le 0.9\varepsilon_{fu}, \tag{44}$$

where ε_{fu} is the FRP design rupture strain. This calculated strain can be used in the moment equation to calculate the moment capacity M_u of the section as follows:

$$M_u = A_s f_s\left(d - \frac{\beta_1 c}{2}\right) + \psi_f A_{frp}\varepsilon_{fd}E_{frp}\left(h - \frac{\beta_1 c}{2}\right) + A_s^{'}f_s^{'}\left(\frac{\beta_1 c}{2} - d'\right), \tag{45}$$

where A_s and A'_s are the cross sectional areas of tensile and compressive steel reinforcement, respectively; f_s and f_s' are the stress in tensile and compressive steel reinforcement, respectively; d and d' are the depths of tensile and compressive steel reinforcement, respectively; h is the overall thickness of the beam; c is the depth of the neutral axis; β_1 is the ratio of depth of equivalent rectangular stress block to depth of the neutral axis; and ψ_f is a reduction factor of 0.85 as recommended by ACI 440 Committee (ACI, 2017). Once the debonding moment capacity of the beam is calculated, the corresponding maximum shear force can be determined to be compared with that determined by the proposed Eqn (33).

To assess the validity of this proposed procedure for predicting the governing debonding failure mode, a database of beams failed by IC debonding was also established. The criteria followed in collecting this database were the same as those followed in collecting the database for the beams failed in PE debonding except the failure mode. The database included 110 beam test results from 30 different studies as given in Table 3. The database included a wide range of design parameters. The dimensions of the beams varied from 115 to 906 mm for the width whereas the height of the beams varied from 100 to 470 mm. The shear span/depth ratio of the beams was in the range of 2.8 to 12.5. The tension steel reinforcement ratio varied from 0.39 to 1.71%. There were 49 beams strengthened with pultruded FRP plates and 61 beams strengthened with wet lay-up FRP sheets. The width of the FRP was in the range of 13 to 480 mm. The thickness of a single layer of dry FRP fibers for the wet lay-up sheets was in the range of 0.11 to 0.572 mm. While the thickness of a single layer of pultruded FRP was in the range of 1.2 to 1.4 mm. The elastic modulus of the FRP materials ranged between 37.2 and 375 GPa. The ratio of the FRP plate length beyond the point load to the shear span was in the range between 0.6 and 1. The compressive strength of concrete ranged between 18.0 and 50.3 MPa. A total of 88 beams were tested in two-point loading system, while 22 beams were tested under one-point loading system.

Equations (33) and (45) were used to predict the shear force corresponding to PE debonding, V_{PED}, and the shear force corresponding to IC debonding, V_{ICD}, respectively, for the beams in the two databases. Table 3 gives the ratio of V_{PED}/V_{ICD} for each beam in each database. For PE debonding database, the procedure is considered to be successful in predicting the occurrence of PE debonding failure when the ratio of V_{PED}/V_{ICD} is less than 1.0. For IC debonding database, the procedure is considered to be successful in predicting the occurrence of IC debonding failure when the ratio of V_{PED}/V_{ICD} is greater than 1.0. Figure 9 plots the ratio of V_{PED}/V_{ICD} against the shear span to depth ratio, a/d, for the two databases. Figure 9a and Table 3 show that the proposed procedure was successful to predict the PE debonding failure for 96.1% of the beams included in the PE debonding database. On the other hand, the proposed procedure successfully predicted the IC debonding failure for 83.6% of the beams included in the IC debonding database as shown in Figure 9b and Table 3. Considering the two databases, the procedure was successful to predict the debonding failure mode for 90.3% of the 238 beams. Also, the ratios of V_{PED}/V_{ICD} for the unsuccessful beams ranged from 1.04 to 1.12 for PE debonding database and from 0.81 to 0.96 for IC debonding database. This result indicates that the error in predicting the actual debonding failure mode is not significant as it ranged from 4 to 19%. As explained earlier, these beams are generally in the transition zone where the PE and IC debonding capacities of the beam are close to each other. Figure 9a shows this transition zone for a/d ratio between 3.0 and 3.6 for the unsuccessful predictions of PE debonding. On the other hand, Figure 9b shows this transition zone for a/d ratio between 3.0 and 4.2 (by excluding the extremes) for the unsuccessful predictions of IC debonding. Considering the entire database, the transition zone of a/d ratio is between 3.0 and 4.2. The occurrence of any of the debonding failures in this zone depends on factors such as beam geometry, amount of tension steel and FRP reinforcements, and concrete strength and cover. Therefore, if the debonding failure mode is required to be predicted to design an anchorage system and the two equations give close prediction loads, it is advisable to apply the anchorage at the critical regions for both PE and IC debonding.

Table 3. Assessment of proposed procedure for prediction of governing debonding failure mode

PE debonding database						IC debonding database						
No.	V_{exp}	Ratio of predicted shear load at PE debonding to that at IC debonding, V_{PED}/V_{ICD}				Reference	Beam	V_{exp}	Ratio of predicted shear load at PE debonding to that at IC debonding, V_{PED}/V_{ICD}			
		Proposed	Teng and Yao (2007)	*fib* Bulletin 14 (2001)	CNR-DT 200 (National Research Council, 2013)				Proposed	Teng and Yao (2007)	*fib* Bulletin 14 (2001)	CNR-DT 200 (National Research Council, 2013)
1	55.4	1.07	1.19	0.73	0.75	Saadatmanesh and Ehsani (1991)	B	125.0	1.16	0.91	0.81	0.84
2	59.6	1.07	1.19	0.73	0.75	Garden et al. (1998)	1U4.5m	30.0	1.35	1.13	0.81	0.79
3	62.9	1.12	1.39	0.74	0.76	Kishi et al. (1998)	A200-1/2	37.0	1.30	3.75	0.90	0.92
4	50.6	0.96	0.87	0.69	0.71		A415-1	41.7	1.21	1.97	0.87	0.89
5	72.0	0.91	0.79	0.67	0.69		A623-1/2	39.5	1.15	1.46	0.85	0.87
6	17.0	0.67	0.74	0.67	0.68		C300-1/2	39.6	1.20	1.98	0.87	0.89
7	12.3	1.04	1.20	0.84	0.80		C445-1/2	42.0	1.15	1.47	0.85	0.87
8	17.5	0.73	0.80	0.72	0.69	Kurihashi et al. (1999)	B0-A	28.1	1.54	1.66	0.90	0.90
9	20.4	0.57	0.56	0.63	0.64		B40-A	26.2	1.54	1.66	0.90	0.90
10	55.0	0.71	0.56	0.62	0.64		B0-A	27.6	1.53	1.66	0.90	0.89
11	45.0	0.69	0.48	0.55	0.57	Takeo et al. (1999)	No. 2	33.9	1.32	1.62	0.80	0.83
12	114.0	1.04	0.74	0.66	0.71		No. 3	38.4	1.14	1.36	0.80	0.83
13	18.3	0.70	0.78	0.69	0.71		No. 4	43.5	1.04	1.23	0.80	0.83
14	17.0	0.76	0.84	0.69	0.71		No. 6	39.3	1.19	1.15	0.73	0.77
15	17.3	0.85	0.94	0.69	0.71		No. 7	42.8	1.11	0.96	0.71	0.75
16	16.0	0.78	0.85	0.74	0.73	Zarnic et al. (1999)	1	58.4	1.27	0.97	0.93	0.90
17	17.8	0.85	0.93	0.74	0.73		2	31.5	2.33	2.18	0.87	0.84
18	15.4	0.95	1.03	0.74	0.73	Bonacci and Maalej (2000)	B2	148.0	0.94	0.94	0.89	0.90
19	16.0	0.67	0.72	0.69	0.67	Kurihashi et al. (2000)	R7-2	35.0	1.43	1.89	0.82	0.85
20	17.0	0.73	0.78	0.69	0.67		R6-2	41.3	1.30	1.67	0.82	0.85
21	17.3	0.81	0.87	0.69	0.67		R5-2	46.5	1.16	1.44	0.82	0.85
22	50.2	0.85	0.70	0.81	0.80		R4-2	58.6	1.01	1.21	0.82	0.85
23	51.1	0.81	0.73	0.74	0.78		R3-2	77.6	0.84	0.97	0.82	0.85
24	50.3	0.81	0.73	0.74	0.78	Matthys (2000)	BF8	111.3	1.09	0.91	0.83	0.77
25	62.1	0.77	0.59	0.64	0.73		BF9	95.8	1.19	1.81	0.92	0.92
26	62.0	0.77	0.59	0.64	0.73	Ceroni et al. (2001)	A2	9.3	1.25	1.30	0.78	0.78
27	68.0	0.87	0.67	0.79	0.79	Chan et al. (2001)	B2	142.5	1.20	0.91	0.81	0.81
28	71.1	0.87	0.67	0.79	0.79		B3	176.0	1.05	0.76	0.85	0.85
29	78.0	0.81	0.56	0.64	0.62		B6	129.0	1.06	0.80	0.81	0.81
30	79.5	0.81	0.56	0.64	0.62		B8	220.0	0.82	0.64	0.88	0.88
31	53.0	0.56	0.49	0.73	0.75	Gao et al. (2001)	1N2	40.4	0.89	1.07	0.81	0.79
32	86.1	0.84	0.88	0.82	0.85	Maeda et al. (2001)	SP-C	39.2	1.09	1.38	0.73	0.78
33	98.2	0.92	0.77	0.88	0.88		SP-C2	54.5	0.96	0.95	0.69	0.74
34	79.3	0.80	0.72	0.82	0.85	Seim et al. (2001)	S11	20.4	2.03	1.65	0.77	0.72
35	41.5	0.68	0.67	0.76	0.77		S1m	21.0	1.78	0.76	0.77	0.72
36	42.9	0.74	0.75	0.76	0.77	Rahimi and Hutchinson (2001)	B3	27.6	1.13	1.23	0.73	0.77
37	48.3	0.85	0.84	0.76	0.77		B4	26.3	1.13	1.23	0.73	0.77
38	55.5	0.87	0.91	0.76	0.77	Spadea et al. (2001)	A1.1	43.4	1.37	1.00	0.87	0.85
39	45.0	0.82	0.82	0.76	0.77		A3.1	37.4	1.31	0.94	0.87	0.85
40	52.0	0.85	0.87	0.76	0.77	Breña et al. (2003)	A3	69.2	1.26	1.06	0.95	0.95
41	52.4	0.81	0.81	0.79	0.79		B1	66.3	1.37	1.02	0.92	0.92
42	59.1	0.78	0.79	0.80	0.81	Kishi et al. (2003)	A250-1	42.1	1.21	2.52	0.87	0.89
43	70.1	0.71	0.72	0.84	0.84		A400-2	80.0	1.08	1.72	0.84	0.86
44	60.3	0.77	0.77	0.81	0.81	Shin and Lee (2003)	R2O	39.4	1.33	1.54	0.98	0.98
45	60.0	0.74	0.67	0.79	0.79		R3O	57.5	1.08	1.30	0.98	0.98
46	62.8	0.71	0.61	0.75	0.76	Takahashi and Sato (2003)	F1	113.5	0.89	1.46	0.83	0.85
47	65.9	0.78	0.78	0.80	0.80		F2	122.0	0.82	0.90	0.78	0.81
48	59.5	0.77	0.76	0.82	0.82		F3	135.0	0.77	0.72	0.75	0.79
49	60.3	0.76	0.74	0.83	0.83		F5	139.0	0.82	0.93	0.75	0.79
50	185.0	0.83	0.64	0.87	0.81		F6	155.5	0.77	0.74	0.72	0.77
51	186.0	0.82	0.64	0.87	0.80	Gao et al. (2004b)	A0	40.4	0.82	1.03	0.84	0.84
52	184.2	0.81	0.62	0.85	0.78	Kotynia (2005)	B-08/S1	90.0	0.85	0.61	0.85	0.79
53	177.0	0.83	0.65	0.88	0.81		BF-04/0.5S	24.0	2.18	1.72	0.85	0.82
54	50.0	0.76	0.64	0.71	0.73		BF-06/S	43.0	1.46	1.09	0.81	0.75
55	51.5	0.76	0.64	0.71	0.73		B-08/M	70.0	1.09	0.77	0.71	0.74
56	48.8	0.72	0.59	0.71	0.73		B-08/S2	47.0	1.46	1.12	0.90	0.88
57	41.0	0.67	0.54	0.71	0.73		B-083m	46.0	1.23	1.30	0.80	0.81
58	43.2	0.80	0.77	0.80	0.76	Maalej and Leong (2005)	C3	326.5	0.81	0.89	0.81	0.90
59	43.2	0.76	0.65	0.78	0.74		C4	334.7	0.81	0.89	0.81	0.90
60	43.0	0.65	0.77	0.82	0.85		C5	325.1	0.78	0.62	0.62	0.72

End of Table 3

PE debonding database						IC debonding database						
No.	V_{exp}	Ratio of predicted shear load at PE debonding to that at IC debonding, V_{PED}/V_{ICD}				Reference	Beam	V_{exp}	Ratio of predicted shear load at PE debonding to that at IC debonding, V_{PED}/V_{ICD}			
		Proposed	Teng and Yao (2007)	*fib* Bulletin 14 (2001)	CNR-DT 200 (National Research Council, 2013)				Proposed	Teng and Yao (2007)	*fib* Bulletin 14 (2001)	CNR-DT 200 (National Research Council, 2013)
61	41.0	0.63	0.63	0.80	0.83	Zhang et al. (2005)	A-1	63.4	1.15	1.29	0.83	0.86
62	39.5	0.61	0.57	0.73	0.81		A-2	63.5	1.17	1.47	0.83	0.86
63	28.1	0.55	0.47	0.77	0.73		A-3	63.1	1.20	1.83	0.83	0.86
64	28.7	0.65	0.54	0.77	0.73		A-4	65.8	1.25	2.81	0.83	0.86
65	29.5	0.71	0.56	0.77	0.73		A-5	62.2	1.19	1.66	0.83	0.86
66	31.0	0.93	0.91	0.66	0.71		A-6	62.1	1.18	1.53	0.83	0.86
67	29.7	0.88	0.80	0.62	0.69		B-2	40.5	1.20	2.41	0.86	0.88
68	32.6	0.93	0.91	0.66	0.71		B-3	42.1	1.22	2.53	0.86	0.88
69	34.9	0.92	0.81	0.62	0.69		B-4	41.1	1.24	2.71	0.87	0.89
70	39.8	0.52	0.51	0.71	0.76		B-6	78.2	1.07	1.65	0.82	0.85
71	66.8	0.71	0.79	0.71	0.76		B-7	79.6	1.09	1.73	0.83	0.86
72	32.1	0.44	0.36	0.66	0.71		B-8	78.1	1.11	1.86	0.84	0.86
73	57.6	0.63	0.66	0.66	0.71		C-1	75.0	0.83	1.03	0.83	0.86
74	53.3	0.57	0.60	0.67	0.72		C-2	76.0	0.82	0.99	0.83	0.85
75	65.3	0.70	0.78	0.67	0.72		C-4	45.3	1.15	1.55	0.83	0.86
76	39.3	0.66	0.56	0.81	0.75		C-5	47.2	1.13	1.48	0.83	0.85
77	35.1	0.66	0.57	0.81	0.75		C-6	48.5	1.10	1.38	0.81	0.84
78	14.0	0.97	1.22	0.80	0.79		C-7	34.4	1.42	2.04	0.83	0.86
79	15.7	0.86	0.94	0.77	0.76		C-8	34.0	1.41	2.07	0.83	0.86
80	19.5	0.79	0.84	0.71	0.71		C-9	35.4	1.36	1.80	0.81	0.84
81	18.4	0.70	0.77	0.66	0.69	Niu et al. (2006)	A1	63.9	2.46	1.37	0.77	0.78
82	17.6	0.69	0.87	0.64	0.70		A2	65.2	2.47	1.37	0.77	0.78
83	20.1	0.83	1.00	0.87	0.86		A3	51.4	2.38	1.48	0.79	0.81
84	22.3	0.76	0.79	0.83	0.83		A4	66.9	2.14	1.04	0.65	0.69
85	24.0	0.72	0.74	0.79	0.79		A5	53.7	2.45	1.29	0.73	0.74
86	26.3	0.66	0.70	0.74	0.76		A6	46.9	2.67	1.76	0.85	0.86
87	24.5	0.66	0.81	0.73	0.77		B1	71.9	1.89	1.07	0.77	0.79
88	58.1	0.65	0.58	0.61	0.67		B2	56.7	1.81	1.16	0.80	0.81
89	68.0	0.63	0.59	0.57	0.64		B3	54.2	2.03	1.38	0.85	0.86
90	66.7	0.67	0.71	0.59	0.66		C2	66.9	2.45	1.38	0.79	0.80
91	40.4	0.82	1.03	0.84	0.84		C3	53.6	2.36	1.49	0.80	0.82
92	43.2	0.75	0.75	0.81	0.80		C4	45.3	2.65	1.77	0.86	0.86
93	68.3	0.78	0.64	0.81	0.81	Aram et al. (2012)	B3	31.4	1.49	1.24	0.79	0.71
94	66.8	0.82	0.87	0.84	0.86		B4	29.2	1.54	1.38	0.81	0.78
95	70.70	0.69	0.58	0.72	0.79	Kotynia et al. (2008)	B-08S	48.0	1.42	1.15	0.91	0.86
96	74.60	0.69	0.58	0.72	0.79		B-08M	70.0	1.11	0.78	0.63	0.66
97	51.40	0.51	0.48	0.72	0.79		B-083m	46.0	1.17	1.31	0.79	0.82
98	53.40	0.51	0.48	0.72	0.79	Al-Negheimish et al. (2012)	PL-1-0.6	126.9	1.38	1.02	0.63	0.65
99	66.00	0.75	0.61	0.68	0.74		PL-1-0.3	87.1	1.68	1.31	0.67	0.68
100	65.20	0.75	0.61	0.68	0.74		PL-2-0.6	115.9	1.65	1.14	0.57	0.57
101	79.00	0.69	0.58	0.72	0.79		S-3-0.2	83.7	1.69	1.34	0.69	0.76
102	61.20	0.69	0.58	0.72	0.79	Hong (2014)	BPS60	32.1	1.58	0.96	0.89	0.78
103	63.30	0.66	0.50	0.62	0.69		BPS90	30.3	2.03	1.73	0.89	0.78
104	63.20	0.66	0.50	0.62	0.69		BPD90	36.9	1.95	1.35	0.71	0.62
105	67.5	0.75	0.61	0.68	0.74		BPDW90	46.5	1.68	1.31	0.76	0.68
106	20.1	0.81	0.62	0.69	0.69	Al-Saawani et al. (2015)	S-0.5-35-240	106.0	1.15	0.87	0.65	0.69
107	35.5	0.82	0.77	0.75	0.79		S-0.9-35-240	129.7	1.05	0.79	0.70	0.73
108	37.2	0.78	0.64	0.73	0.77		S-1.3-35-240	153.1	0.96	0.72	0.73	0.76
109	54.3	0.70	0.74	0.76	0.79		S-0.9-24-240	125.2	1.04	0.75	0.69	0.71
110	52.3	0.67	0.60	0.70	0.77		SN-0.9-35-240	130.4	1.07	0.80	0.74	0.77
111	53.9	0.81	0.90	0.80	0.81							
112	50.7	0.63	0.49	0.62	0.64							
113	20.0	0.86	0.83	0.79	0.82							
114	24.6	0.71	0.93	0.86	0.88							
115	24.1	0.66	0.68	0.82	0.85							
116	30.4	0.62	0.46	0.54	0.58							
117	23.5	0.53	0.41	0.54	0.58							
118	26.0	0.39	0.25	0.50	0.57							
119	37.9	0.64	0.89	0.72	0.77							
120	117.5	0.97	0.70	0.62	0.65							
121	50.0	0.79	0.70	0.63	0.62							
122	50.8	0.79	0.70	0.63	0.62							
123	39.5	0.67	1.08	0.78	0.82							
124	39.0	0.67	1.08	0.78	0.82							
125	39.8	0.67	1.08	0.78	0.82							
126	34.0	0.66	1.05	0.82	0.85							
127	22.0	0.83	0.96	0.68	0.73							
128	24.0	0.83	0.96	0.68	0.73							
Successful Predictions		96.1%	90.6%	100.0%	100.0%	Successful Predictions			83.6%	72.7%	0.0%	0.0%

Note: V_{ICD} was calculated based on ACI 440 IC debonding equation.

The comparison with the experimental databases indicated that the proposed procedure can be reliably used for predicting the governing debonding failure mode of FRP strengthened beams. To further verify the proposed procedure, selected PE debonding equations can be used instead of the proposed PE equation. In this verification, the equations of Teng and Yao (2007), *fib* Bulletin 14 (*fib*, 2001), and Italian code CNR-DT 200 (National Research Council, 2013) were selected. The selection of these three equations was made because the former provided the best predictions of the shear based models while the latter two provided the best predictions of fracture energy approach as presented previously in the paper. Each of the three models was combined with the IC debonding equation of the ACI 440.2R (ACI, 2017) guidelines to calculate the ratio of V_{PED}/V_{ICD} for each beam in the two databases as given in Table 3. Figures 10 through 12 show the variation of the ratio of V_{PED}/V_{ICD} with the shear span to depth ratio using the three different PE models. As can be seen from Table 3 and Figure 10, the procedure considering Teng and Yao's model (2007) was successful to predict the PE debonding mode of failure for 90.6% of the beams included in the database. The percentage was reduced to 72.7% for the IC debonding database. The procedures considered *fib* Bulletin 14 (*fib*, 2001) and Italian code CNR-DT 200 (National Research Council, 2013) were successful to predict the PE debonding mode of failure for all beams in the database as shown in Table 3 and Figures 11 and 12. On the other hand, the table and the figures show that both code methods were not able to predict the

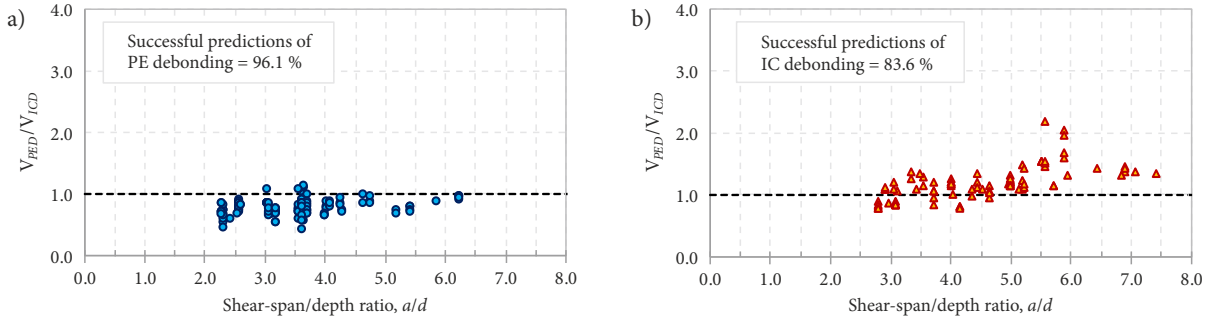

Figure 9. Prediction of the governing debonding failure mode using the proposed PE debonding equation and ACI 440 IC debonding equation: a – PE debonding database; b – IC debonding database

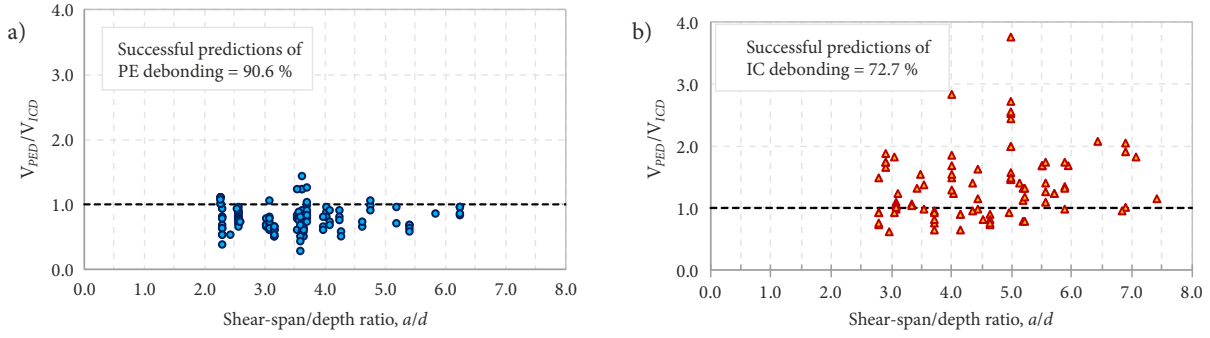

Figure 10. Prediction of the governing debonding failure mode using Teng and Yao (2007) PE debonding model and ACI 440 IC debonding equation: a – PE debonding database; b – IC debonding database

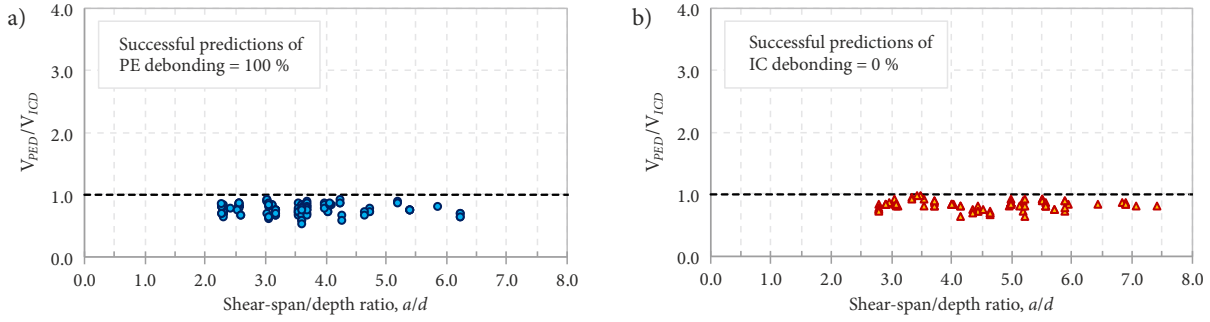

Figure 11. Prediction of the governing debonding failure mode using *fib* Bulletin 14 (*fib*, 2001) PE debonding model and ACI 440 IC debonding equation: a – PE debonding database; b – IC debonding database

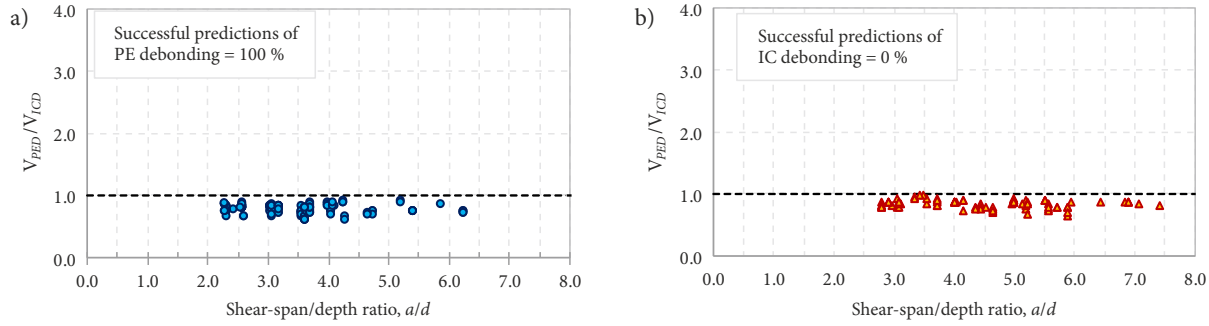

Figure 12. Prediction of the governing debonding failure mode using CNR-DT 200 (National Research Council, 2013) PE debonding model and ACI 440 IC debonding equation: a – PE debonding database; b – IC debonding database

IC debonding failure mode for any of the beams in the database. This is attributed to the fact that the predictions of the two methods are based on predicting the debonding strain ε_{fd} corresponding to PE debonding failure which is always smaller than the IC debonding strain. This made the calculated V_{PED} by the two methods less than the calculated V_{ICD} for each beam in the database. This comparison indicates that the procedure with the proposed PE debonding equation provided more reliable and correct predictions for the debonding failure mode.

Conclusions

A proposed model for predicting PE debonding capacity of FRP strengthened RC beams was presented. The model was formulated empirically based on the concrete shear strength of the beams. The main parameters affecting the PE debonding capacity were considered in the model. Based on the research presented in this paper, the following conclusions can be drawn:

- The proposed model was used to predict the PE debonding capacity of 128 FRP strengthened RC beams from 32 different studies available in the literature. It was found that the proposed model provided accurate and conservative predictions over the range of variables known to affect the PE debonding capacity of the beams.
- The proposed model was compared to the existing shear based and fracture energy based models using the available test data. The comparison indicated that the proposed model gave more accurate and consistent predictions, yet simpler than most of the existing models.
- The proposed model was combined with the ACI 440 IC debonding model to allow predict the governing debonding failure mode of FRP strengthened RC beams. The validity of the combination was verified using two experimental databases for beams failed in PE debonding or IC debonding. Furthermore, the proposed combination was found to be more reliable in predicting the debonding failure mode than other code combinations.

Acknowledgements

The authors would like to thank Deanship of Scientific Research for funding and supporting this research through the initiative of DSR Graduate Students Research Support (GSRS) at King Saud University, Saudi Arabia.

Author contributions

All authors have contributed equally.

Disclosure statement

The authors declare that they have no conflict of interest in this article.

References

Achintha, M., & Burgoyne, C. J. (2011). Fracture mechanics of plate debonding: Validation against experiment. *Construction and Building Materials*, *25*(6), 2961–2971. https://doi.org/10.1016/j.conbuildmat.2010.11.103

Achintha, P. M. M., & Burgoyne, C. J. (2008). Fracture mechanics of plate debonding. *Journal of Composites for Construction*, *12*(4), 396–404. https://doi.org/10.1061/(ASCE)1090-0268(2008)12:4(396)

Ahmed, O. A. F. (2000). *Strengthening of R. C. beams by means of externally bonded CFRP laminates: Improved model for plate-end shear* [PhD Thesis]. Department of Civil Engineering, Catholicke University of Leuven, Belgium.

Ahmed, O., & Van Gemert, D. (1999). Effect of longitudinal carbon fiber reinforced plastic laminates on shear capacity of reinforced concrete beams. *Proceedings of the Fourth International Symposium on Fiber Reinforced Polymer Reinforcement for Reinforced Concrete Structures*. Maryland, USA.

Alfano, G., De Cicco, F., & Prota, A. (2012). Intermediate debonding failure of RC beams retrofitted in flexure with FRP: experimental results versus predictions of codes of practice. *Journal of Composites for Construction*, *16*(2), 185–195. https://doi.org/10.1061/(ASCE)CC.1943-5614.0000250

Al-Negheimish, A., El-Sayed, A., Al-Zaid, R., Shuraim, A., & Alhozaimy, A. (2012). Behavior of wide shallow RC beams strengthened with CFRP reinforcement. *Journal of Composites for Construction*, *16*(4), 418–429. https://doi.org/10.1061/(ASCE)CC.1943-5614.0000274

Al-Saawani, M., El-Sayed, A., & Al-Negheimish, A. (2015). Effect of basic design parameters on IC debonding of CFRP-strengthened shallow RC beams. *Journal of Reinforced Plastics and Composites*, *34*(18), 1526–1539. https://doi.org/10.1177/0731684415593816

Al-Tamimi, A., Hawileh, R. J., & Rasheed, H. (2011). Effects of ratio of CFRP plate length to shear span and end anchorage on flexural behavior of SCC RC beams. *Journal of Composites and Construction*, *15*(6), 908–919. https://doi.org/10.1061/(ASCE)CC.1943-5614.0000221

American Concrete Institute. (2002). *Guide for the design and construction of externally bonded FRP systems for strengthening concrete structures* (ACI 440.2R). Farmington Hills, Michigan, USA.

American Concrete Institute. (2014). *Building code requirements for structural concrete and commentary* (ACI 318). Farmington Hills, USA.

American Concrete Institute. (2017). *Guide for the design and construction of externally bonded FRP systems for strengthening concrete structures* (ACI 440.2R). Farmington Hills, Michigan, USA.

Aram, M., Czaderski, C., & Motavalli, M. (2012). Debonding failure modes of flexural FRP-strengthened RC beams. *Composites Part B: Engineering*, *39*, 826–841. https://doi.org/10.1016/j.compositesb.2007.10.006

Arduini, M., Di Tommaso, A., & Nanni, A. (1997). Brittle failure in FRP plate and sheet bonded beams. *ACI Structural Journal*, *94*(4), 363–370. https://doi.org/10.14359/487

Beber, A. J., Filho, A. C., & Campagnolo, J. L. (1999). Flexural strengthening of R/C beams with CFRP sheets. *Proceedings of the Eighth International Conference on Advanced Composites for Concrete Repair*, London, UK.

Benjeddou, O., Ouezdou, M. B., Bedday, A. (2007). Damaged RC beams repaired by bonding of CFRP laminates. *Construction and Building Materials*, *21*, 1301–1310. https://doi.org/10.1016/j.conbuildmat.2006.01.008

Blaschko, M. (1997). Strengthening with CFRP. In *Münchner Massivbau Seminar*, TU München (in German).

Bonacci, J. F., & Maalej, M. (2000). Externally bonded fiber-reinforced polymer for rehabilitation of corrosion damaged concrete beams. *ACI Structural Journal*, *97*(5), 703–711. https://doi.org/10.14359/8805

Breña, S. F., & Macri, B. M. (2004). Effect of carbon-fiber-reinforced polymer laminate configuration on the behavior of strengthened reinforced concrete beams. *Journal of Composites for Construction*, *8*(3), 229–240. https://doi.org/10.1061/(ASCE)1090-0268(2004)8:3(229)

Breña, S., Bramblett, R., Wood, S., & Kreger, M. (2003). Increasing flexural capacity of reinforced concrete beams using carbon fiber-reinforced polymer composites. *ACI Structural Journal*, *100*(1), 36–46. https://doi.org/10.14359/12437

Ceroni, F. (2010). Experimental performances of RC beams strengthened with FRP materials. *Construction and Building Materials*, *24*, 1547–1559. https://doi.org/10.1016/j.conbuildmat.2010.03.008

Ceroni, F., Manfredi, G., & Pecce, M. (2001). Crack widths in RC beams strengthened with carbon fabrics. *Proceedings of FRPRCS-5*, Cambridge.

Chan, T. K., Cheong, H. K., & Nguyen, D. M. (2001). Experimental investigation on delamination failure of CFRP strengthened beams. In *Proceedings of ICCMC/IBST International Conference on Advanced Technologies in Design, Construction, and Maintenance of Concrete Structures*, Hanoi, Vietnam.

Colotti, V., Spadea, G., & Swamy, R. N. (2004). Structural model to predict the failure behavior of plated reinforced concrete beams. *Journal of Composites for Construction*, *8*(2), 104–122. https://doi.org/10.1061/(ASCE)1090-0268(2004)8:2(104)

Concrete Society. (2012). *Design guidance for strengthening concrete structures using fibre composite materials* (Technical Report No. 55). Crowthorne, UK.

David, E., Djelal, C., Ragneau, E., & Bodin, F. B. (1999). Use of FRP to strengthen and repair RC beams: experimental study and numerical simulations. In *Proceedings of the Eighth International Conference on Advanced Composites for Concrete Repair*, London, UK.

El-Sayed, A. K. (2014). Effect of longitudinal CFRP strengthening on the shear resistance of reinforced concrete beams. *Journal of Composites Part B: Engineering*, *58*, 422–429. https://doi.org/10.1016/j.compositesb.2013.10.061

Esfahani, M. R., Kianoush, M. R., & Tajari, A. R. (2007). Flexural behavior of reinforced concrete beams strengthened by CFRP sheets. *Engineering Structures*, *29*, 2428–2444. https://doi.org/10.1016/j.engstruct.2005.09.011

European Committee for Standardization. (2004). *Eurocode 2: Design of concrete structures – Part 1-1: General rules and rules for buildings* (EN 1992-1-1).

Fanning, P. J., & Kelly, O. (2001). Ultimate response of RC beams strengthened with CFRP plates. *Journal of Composites for Construction*, *5*(2), 122–127. https://doi.org/10.1061/(ASCE)1090-0268(2001)5:2(122)

Gao, B., Kim, J. K., & Leung, C. K. Y. (2004a). Taper ended FRP strips bonded to RC beams: Experiments and FEM analysis. In *Proceedings of the Second International Conference on FRP in Civil Engineering* (pp. 399–405). https://doi.org/10.1201/9780203970850.ch43

Gao, B., Kim, J. K., & Leung, C. K. Y. (2004b). Experimental study on RC beams with FRP strips bonded with rubber modified resins. *Composite Science and Technology*, *64*, 2557–2564. https://doi.org/10.1016/j.compscitech.2004.05.016

Gao, B., Leung, W., Cheung, C., Kim, J. K., & Leung, C. K. Y. (2001). Effects of adhesive properties on strengthening of concrete beams with composite strips. In *Proceedings of the International Conference on FRP composites in Civil Engineering* (pp. 423–432). Elsevier.

Garden, H. N., Hollaway, L. C., & Thorne, A. M. (1997). A preliminary evaluation of carbon fibre reinforced polymer plates for strengthening reinforced concrete members. *Proceedings of the Institution of Civil Engineers: Structures and Buildings*, *123*, 127–142. https://doi.org/10.1680/istbu.1997.29302

Garden, H. N., Quantrill, R. J., Hollaway, L. C., Thorne, A. M., & Parke, G. A. R. (1998). An experimental study of the anchorage length of carbon fiber composite plates used to strengthen reinforced concrete beams. *Construction and Building Materials*, *12*(4), 203–219. https://doi.org/10.1016/S0950-0618(98)00002-6

Grace, N. F., & Singh, S. B. (2005). Durability evaluation of carbon fiber-reinforced polymer strengthened concrete beams: experimental study and design. *ACI Structural Journal*, *102*(1), 40–48. https://doi.org/10.14359/13529

Hasnat, A., Islam, M., & Amin, A. (2016). Enhancing the debonding strain limit for CFRP-strengthened RC beams using U-clamps: Identification of design parameters. *Journal Composites Construction*, *20*(1), 04015039-1–04015039-16. https://doi.org/10.1061/(ASCE)CC.1943-5614.0000599

Hau, K. M. (1999). *Experiments on concrete beams strengthened by bonding fibre reinforced plastic sheets* [MSc in Civil Engineering thesis]. The Hong Kong Polytechnic University, Hong Kong, China.

Hong, S. (2014). Effect of intermediate crack debonding on the flexural strength of CFRP-strengthened RC beams. *Mechanics of Composite Materials*, *50*(4), 523–536. https://doi.org/10.1007/s11029-014-9439-6

International Federation for Structural Concrete. (2001). *Externally bonded FRP reinforcement for RC structures* (fib Bulletin 14). Lausanne, Switzerland.

Jansze, W. (1997). *Strengthening of RC members in bending by externally bonded steel plates* [PhD thesis]. Delft University of Technology.

Kani, G. N. J. (1999). Basic facts concerning shear failure. *ACI Journal Proceedings*, *63*(6), 675–692.

Kishi, N., Mikami, H., & Zhang, G. (2003). Numerical analysis of debonding behavior of FRP sheet for flexural strengthening RC beams. *Proceedings of Japan Society of Civil Engineers*, 255–272. https://doi.org/10.2208/jscej.2003.725_255

Kishi, N., Mikami, H., Sato, M., & Matsuoka, K. (1998). Bending bond strength of RC beams strengthened with FRP sheet. *Procurement of Japan Concrete Institute*, *20*, 515–520.

Kotynia, R. (2005). Debonding failures of RC beams strengthened with externally bonded strips. *Proceedings of the International Symposium on Bond Behavior of FRP in Structures*, 247–252.

Kotynia, R., Abdel Baky, H., Neale, K., Ebead, U. (2008). Flexural strengthening of RC beams with externally bonded CFRP systems: Test results and 3D nonlinear FE analysis. *Journal of Composites for Construction*, *12*(2), 190–201. https://doi.org/10.1061/(ASCE)1090-0268(2008)12:2(190)

Kurihashi, Y., Kishi, N., Mikami, H., Matsuoka, K. (1999). Flexurally bonding property of FRP sheet on RC beam with two-point loading. *Procurement of Japan Concrete Institute*, *21*, 1555–1560.

Kurihashi, Y., Kishi, N., Mikami, H., & Matsuoka, K. (2000). Sheet volume effects on flexural bonding property of RC beams strengthened with FRP sheet. *Proceedings of Japan Concrete Institute*, *22*, 481–486.

Maalej, M., & Bian, Y. (2001). Interfacial shear stress concentration in FRP-strengthened beams. *Composite Structures*, *54*, 417–426. https://doi.org/10.1016/S0263-8223(01)00078-2

Maalej, M., & Leong, K. S. (2005). Effect of beam size and FRP thickness on interfacial shear stress concentration and failure mode of FRP-strengthened beams. *Composite Science and Technology*, *65*(7–8), 1148–1158. https://doi.org/10.1016/j.compscitech.2004.11.010

Maeda, T., Komaki, H., Tsubouchi, K., & Murakami, K. (2001). Strengthening behavior of carbon fiber sheet using flexible layer. *Proceedings of Japan Concrete Institute*, *23*, 817–822.

Matthys, S. (2000). *Structural behavior and design of concrete beams strengthened with externally bonded FRP reinforcement* [PhD thesis]. Ghent University.

National Research Council. (2013). *Guide for the design and construction of externally bonded FRP systems for strengthening existing structures* (CNR-DT 200 R1). Rome, Italy.

Nguyen, D. M., Chan, T. K., & Cheong, H. K. (2001). Brittle failure and bond development length of CFRP–concrete beams. *Journal of Composites for Construction*, *5*(1), 12–17. https://doi.org/10.1061/(ASCE)1090-0268(2001)5:1(12)

Niu, H., Vasquez, A., Karbhari, V. M. (2006). Effect of material configuration on strengthening of concrete slabs by CFRP composites. *Composites Part B: Engineering*, *37*(2–3), 213–226. https://doi.org/10.1016/j.compositesb.2005.05.015

Oehlers, D. J. (1992). Reinforced concrete beams with plates glued to their soffits. *Journal of Structural Engineering*, *118*(8), 2023–2038. https://doi.org/10.1061/(ASCE)0733-9445(1992)118:8(2023)

Oehlers, D. J., Liu, I. S. T., & Seracino, R. (2005). Shear deformation debonding of adhesively bonded plates. *Proceedings of the Institution of Civil Engineers: Structures and Buildings*, *158*(1), 77–84. https://doi.org/10.1680/stbu.2005.158.1.77

Oehlers, D. J., Liu, I. S. T., Seracino, R., & Mohamed Ali, M. S. (2004). Prestress model for shear deformation debonding of FRP- and steel-plated RC beams. *Magazine of Concrete Research*, *56*(8), 475–486. https://doi.org/10.1680/macr.2004.56.8.475

Pham, H. B., & Al-Mahaidi, R. (2006). Prediction models for debonding failure loads of carbon fiber reinforced polymer retrofitted reinforced concrete beams. *Journal of Composites for Construction*, *10*(1), 48–59. https://doi.org/10.1061/(ASCE)1090-0268(2006)10:1(48)

Quantrill, R. J., Hollaway, L. C., & Thorne, A. M. (1996). Experimental and analytical investigation of FRP strengthened beam response: Part I. *Magazine of Concrete Research*, *48*, 331–342. https://doi.org/10.1680/macr.1996.48.177.331

Rahimi, H., & Hutchinson, A. (2001). Concrete beams strengthened with externally bonded FRP plates. *Journal of Composites for Construction*, *5*(1), 44–56. https://doi.org/10.1061/(ASCE)1090-0268(2001)5:1(44)

Rebeiz, K. S. (1999). Shear strength prediction for concrete members. *Journal of Structural Engineering*, *125*(3), 301–308. https://doi.org/10.1061/(ASCE)0733-9445(1999)125:3(301)

Ritchie, P. A., Thomas, D. A., Lu, L. W., & Conelly, G. M. (1991). External reinforcement of concrete beams using fibre reinforced plastics. *ACI Structural Journal*, *88*(4), 490–500. https://doi.org/10.14359/2723

Saadatmanesh, H., & Ehsani, M. R. (1991). RC beams strengthened with GFRP plates I: experimental study. *Journal of Structural Engineering*, *117*(11), 3417–3433. https://doi.org/10.1061/(ASCE)0733-9445(1991)117:11(3417)

Sadrmomtazi, A., Rasmi Atigh, H., & Sobhan, J. (2014). Experimental and analytical investigation on bond performance of the interfacial debonding in flexural strengthened RC beams with CFRP sheets at tensile face. *Asian Journal of Civil Engineering* (*BHRC*), *15*(3), 391–410.

Sakr, M. A. (2018). Finite element modeling of debonding mechanisms in carbon fiber reinforced polymer-strengthened reinforced concrete continuous beams. *Structural Concrete*, *19*(4), 1002–1012. https://doi.org/10.1002/suco.201700011

Seim, W., Horman, M., Karbhari, V., & Seible, F. (2001). External FRP post-strengthening of scaled concrete slabs. *Journal of Composites for Construction*, *5*(2), 67–75. https://doi.org/10.1061/(ASCE)1090-0268(2001)5:2(67)

Shin, Y. S., & Lee, C. (2003). Flexural behavior of reinforced concrete beams strengthened with carbon fiber-reinforced polymer laminates at different levels of sustaining load. *ACI Structural Journal*, *100*(2), 231–239. https://doi.org/10.14359/12487

Skuturna, T., & Valivonis, J. (2016). Experimental study on the effect of anchorage systems on RC beams strengthened using FRP. *Composites Part B: Engineering*, *91*, 283–290. https://doi.org/10.1016/j.compositesb.2016.02.001

Smith, S. T., & Teng, J. G. (2002a). FRP-strengthened RC beams. I: Assessment of debonding strength models. *Engineering Structures*, *24*(4), 385–395. https://doi.org/10.1016/S0141-0296(01)00105-5

Smith, S. T., & Teng, J. G. (2002b). FRP-strengthened RC beams. II: Assessment of debonding strength models. *Engineering Structures*, *24*(4), 397–417. https://doi.org/10.1016/S0141-0296(01)00106-7

Smith, S. T., & Teng, J. G. (2003). Shear-bending interaction in debonding failures of FRP-plated RC beams. *Advances in*

Structural Engineering, *6*(3), 183–199. https://doi.org/10.1260/136943303322419214

Spadea, G., Swamy, R. N., Bencardino, F. (2001). Strength and ductility of RC beams repaired with bonded CFRP laminates. *Journal of Bridge Engineering*, *6*(5), 349–355. https://doi.org/10.1061/(ASCE)1084-0702(2001)6:5(349)

Standards Australia. (1988). *Concrete structures* (AS 3600). Sydney, Australia.

Standards Australia. (2017a). *Bridge design*, *Part 5: Concrete* (AS 5100.5). SA1 Global Limited, Australia.

Standards Australia. (2017b). *Bridge design, Part 8: Rehabilitation and strengthening of existing bridges* (AS 5100.8). SA1 Global Limited, Australia.

Takahashi, Y., & Sato, Y. (2003). Flexural behavior of RC beams externally reinforced with carbon fiber sheets. In *Proceedings of FRPRCS-6 – Fibre-reinforced Polymer Reinforcement for Concrete Structures* (pp. 237–246). https://doi.org/10.1142/9789812704863_0020

Takeo, K., Matsushita, H., Sagawa, Y., & Ushigome, T. (1999). Experiment of RC beam reinforced with CFRP adhesive method having variety of shear-span ratio. *Procurement of Japan Concrete Institute*, *21*, 205–210.

Teng, J. G., & Yao, J. (2007). Plate end debonding in FRP-plated RC beams – II: Strength model. *Engineering Structures*, *29*(10), 2472–2486. https://doi.org/10.1016/j.engstruct.2006.11.023

Tumialan, G., Serra, P., Nanni, A., & Belarbi, A. (1999). Concrete cover delamination in reinforced concrete beams strengthened with carbon fiber reinforced polymer sheets. In *Proceedings of the Fourth International Symposium on Fiber Reinforced Polymer Reinforcement for Reinforced Concrete Structures* (pp. 725–735). Maryland, USA.

Valcuende, M., Benlloch, J., & Parra, C. J. (2003). Ductility of reinforced concrete beams strengthened with CFRP strips and fabric. In *Proceedings of the Sixth International Symposium on FRP Reinforcement for Concrete Structures* (pp. 337–346). https://doi.org/10.1142/9789812704863_0030

Yao, J., & Teng, J. G. (2007). Plate end debonding in FRP-plated RC beams – I: Experiments. *Engineering Structures*, *29*(10), 2457–2471. https://doi.org/10.1016/j.engstruct.2006.11.022

Zarnic, R., Gostic, S., Bosiljkov, V., & Bokan-Bosiljkov, V. (1999). Improvement of bending load-bearing capacity by externally bonded plates. In *Proceedings of Creating with Concrete* (pp. 433–442). https://doi.org/10.1680/stamfcc.28258.0041

Zhang, G. F., Kishi, N., Mikami, H., & Komuro, M. (2005). A numerical prediction method for flexural behavior of RC beams reinforced with FRP sheet. In *Proceedings of the International Symposium on Bond Behaviour of FRP in Structures* (pp. 215–220).

Zhang, S. S., & Teng, J. G. (2016). End cover separation in RC beams strengthened in flexure with bonded FRP reinforcement: simplified finite element approach. *Materials and Structures*, *49*, 2223–2236. https://doi.org/10.1617/s11527-015-0645-z

Zhang, S. S., & Teng, J. G. (2014). Finite element analysis of end cover separation in RC beams strengthened in flexure with FRP. *Engineering Structures*, *75*, 550–560. https://doi.org/10.1016/j.engstruct.2014.06.031

Zsutty, T. (1971). Shear strength prediction for separate categories of simple beam tests. *ACI Structural Journal*, *68*(2), 138–143. https://doi.org/10.14359/11300